Stability of crack fronts under Griffith criterion: a computational approach using integral equations and domain derivatives of potential energy

Marc Bonnet

Stability of crack fronts under Griffith criterion: a computational approach using integral equations and domain derivatives of potential energy

Marc Bonnet*

Laboratoire de Mécanique des Solides (UMR CNRS 7649), Ecole Polytechnique, 91128 Palaiseau cedex, France

This paper deals with the numerical study of stability and instantaneous extension of cracks under Griffith criterion, within the classical linear fracture mechanics framework. First- and second-order domain derivatives of the potential energy W in crack extensions play a central role in the mathematical formulation of such situations. The proposed solution strategy (called the θ-integral method, by reference to the FEM-based θ-method) possesses the following main characteristics: (i) it is based on a symmetric Galerkin boundary integral formulations; and (ii) explicit expressions for the domain derivatives of W are established using Lagrangian formulas (so that the derivations do not increase crack front singularities). The numerical solution procedure for the extension velocity problem, including all domain derivative evaluations, is entirely supported by the boundary element mesh of the current crack configuration; numerical differentiation is avoided. Numerical examples for an isolated crack in a 3-D unbounded elastic body show that in practice an excellent accuracy can be achieved for the energy release rate, the second-order domain derivatives of W and the prediction of stability or instability of crack growth.

1. Introduction

In the classical Griffith approach, crack propagation may occur at points of the crack front where the energy release rate G reaches a critical value G_c. For a quasi-static loading history and assuming infinitesimal displacements and strains, the governing problem for the extension velocity of the crack front on the current configuration has been formulated as a variational inequality [16,17]. Mathematically speaking, G is (minus) the kernel associated with the domain derivative of the equilibrium value W of the potential energy. Then, the variational inequality, and in particular the stability and non-bifurcation criteria, involves the second-order domain derivative of W.

The consideration of perturbations of W under fictitious body changes associated to virtual crack extensions provides a computational tool for fracture analysis. Finite difference approaches, using small finite crack perturbations, have been proposed using either FEM [12,21] or BEM [8,7, pp. 50–55]. Then, the concept of material differentiation (i.e. analytical differentiation using infinitesimal crack perturbations) has been applied to W, starting from variational formulations of elasticity problems [9,10,14,18,20,25]. This approach, sometimes known as the 'θ-method' (θ refers to the notation used in [10,14] and herein for the transformation velocity), has led to FEM implementations [27]. The present paper aims at formulating a BIE version of the θ-method.

This paper aims at developing a solution strategy for the governing variational inequality whose main characteristics are: (i) a boundary integral equation (BIE) framework, reflecting the major role played by the

* E-mail: bonnet@lms.polytechnique.fr

crack surface and its perturbations; (ii) the recourse to explicit expressions for the domain derivatives of W, avoiding any numerical differentiation. This approach, herein referred to as the θ-integral method, is in fact a transposition to boundary integral equation formulations of the θ-method. More specifically, symmetric Galerkin BIEs [6,15] are used here because, like in FEM, their symmetry allows one to formulate second-order derivatives of W in terms of the elastic field variables and their first-order domain derivatives. The present development, like the classical θ-method, relies on Lagrangian-type domain differentiation formulas, in order to avoid the appearance of non-integrable crack front singularities during the differentiation process. The resulting solution procedure for the extension velocity problem is entirely supported by the boundary element discretisation (assuming linear elasticity). Numerical examples for an isolated crack in a 3-D unbounded elastic body are presented in Section 7. They show that, in practice, an excellent accuracy can be achieved for G, the second-order domain derivatives of W and the prediction of stability or instability of crack growth. Although the Griffith criterion alone is insufficient for mixed-mode three-dimensional crack propagation simulation, our approach could be combined with other techniques in more complex propagation criteria.

2. Lagrangian differentiation in crack perturbations

Let Ω denote a three-dimensional elastic solid. The boundary $\partial\Omega$ of Ω is split into two components S_u (supporting prescribed displacements $\boldsymbol{u} = \bar{\boldsymbol{u}}$) and S_T (supporting prescribed tractions $\boldsymbol{\sigma}.\boldsymbol{n} = \bar{\boldsymbol{t}}$, see Fig. 1). A crack, idealized by the surface Γ, is embedded into Ω. The unit normal $\boldsymbol{n}$ to Γ is oriented along the $\Gamma^- \to \Gamma^+$ direction, where Γ^+, Γ^- are the two crack faces (the outward normal to $\Gamma^\pm$ is thus $\mp\boldsymbol{n}$).

The crack edge $\partial\Gamma$ is a closed, generally nonplanar, curve; let $\boldsymbol{\tau}(s)$ denote the unit tangent vector to $\partial\Gamma$ (s: arc length along $\partial\Gamma$). Then, let $\boldsymbol{\nu} = \boldsymbol{\tau} \wedge \boldsymbol{n}$ denote the outward unit normal to $\partial\Gamma$ lying in the tangent plane to Γ, so that $(\boldsymbol{\tau}, \boldsymbol{n}, \boldsymbol{\nu})$ is an orthonormal right-handed frame. The components of a vector $\boldsymbol{\theta}$ in $(\boldsymbol{\tau}, \boldsymbol{n}, \boldsymbol{\nu})$ will be denoted $(\theta_\tau, \theta_n, \theta_\nu)$:

$$\boldsymbol{\theta} = \theta_\tau \boldsymbol{\tau} + \theta_n \boldsymbol{n} + \theta_\nu \boldsymbol{\nu} \tag{1}$$

Smooth crack perturbations (i.e. without kinking) are considered, so that the vector $\boldsymbol{\nu}$ defines the instantaneous crack extension direction.

Crack extensions may be mathematically described using a pseudo-time $t \geq 0$ and a geometrical transformation $\boldsymbol{\Phi}$:

$$\boldsymbol{x} \in \Omega \to \boldsymbol{x}' = \boldsymbol{\Phi}(\boldsymbol{x}, t) \in \Omega(t) \tag{2}$$

which must satisfy

$$\boldsymbol{\Phi}(\Omega, t) = \Omega \qquad \boldsymbol{\Phi}(\Gamma, t) \supset \Gamma \tag{3}$$

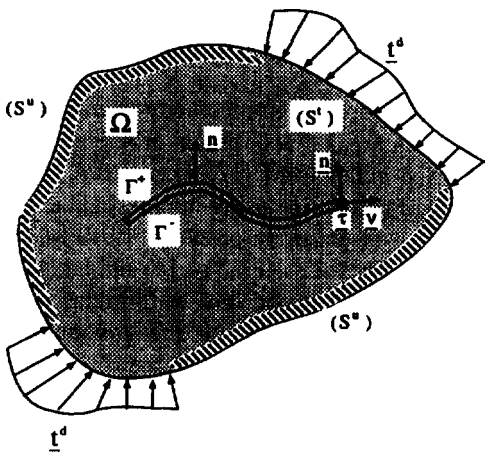

Fig. 1. Cracked elastic solid Ω.

Here, *instantaneous* crack extensions are considered, so that the unperturbed crack configuration corresponds conventionally to $t = 0$, and all derivatives will be implicitly taken at $t = 0$.

Differentiation of field variables and integrals in a domain perturbation is a well-documented subject, see e.g. [22,24]; a few basic facts are recalled now [4]. The *initial transformation velocity* $\boldsymbol{\theta}$ is defined by

$$\boldsymbol{\theta}(\boldsymbol{x}) = \left.\frac{\partial \boldsymbol{\Phi}}{\partial t}\right|_{t=0}$$

The 'Lagrangian' derivative at $t = 0$ of a field quantity $f(\boldsymbol{y}, t)$ in a geometrical transformation, denoted by $\overset{*}{f}$, is defined by

$$\overset{*}{f} = \lim_{t \searrow 0} \frac{1}{t}\,[f(\boldsymbol{x}' - f(\boldsymbol{x}, 0)] = \frac{\partial f}{\partial t} + \nabla f \,.\, \boldsymbol{\theta} \tag{4}$$

The Lagrangian derivative of the gradient of a field quantity is then given by

$$(\nabla f)* = \nabla \overset{*}{f} - \nabla f \,.\, \nabla \boldsymbol{\theta} \tag{5}$$

where the symbol '.' indicates the dot product of two vectors or tensors (e.g. $\nabla f \,.\, \nabla \boldsymbol{\theta} = f_{,i}\theta_{i,j}\boldsymbol{e}_j$). Similarly, the Lagrangian derivative of any surface integral of the form

$$I(f, S; t) = \int_{S(t)} f \, \mathrm{d}S$$

is given by the formula

$$\overset{*}{I}(f, S) = \frac{\mathrm{d}I}{\mathrm{d}t} = \int_S \overset{*}{f} \, \mathrm{d}S + \int_S f \, \mathrm{div}_S \, \boldsymbol{\theta} \, \mathrm{d}S \tag{6}$$

where the surface divergence of a vector field is defined by

$$\mathrm{div}_S(\,) \equiv \mathrm{div}(\,) - \boldsymbol{n} \,.\, \nabla(\,) \,.\, \boldsymbol{n} \tag{7}$$

Note that $\overset{*}{f}$ and $\overset{*}{I}$ are linear expressions in $\boldsymbol{\theta}$ if $\partial f / \partial t = 0$.

From formula (6), the Lagrangian derivative of a double surface integral is given by

$$\frac{\mathrm{d}}{\mathrm{d}t} \int_\Gamma \int_\Gamma f(\boldsymbol{x}, \boldsymbol{y}) \, \mathrm{d}S_x \, \mathrm{d}S_y = \int_\Gamma \int_\Gamma \{\overset{*}{f}(\boldsymbol{x}, \boldsymbol{y}) + f(\mathrm{div}_S \, \boldsymbol{\theta}(\boldsymbol{x}) + \mathrm{div}_S \, \boldsymbol{\theta}(\boldsymbol{y}))\} \, \mathrm{d}S_x \, \mathrm{d}S_y \tag{8}$$

Finally, the Lagrangian derivative of a integral over a line C is given by

$$\frac{\mathrm{d}}{\mathrm{d}t} \int_C f \, \mathrm{d}s = \int_C \left\{ \overset{*}{f} + f\left[\frac{\mathrm{d}}{\mathrm{d}s}(\theta_\tau) - \kappa \theta_m \right] \right\} \mathrm{d}s \tag{9}$$

(κ: algebraic curvature of C; $\boldsymbol{m}$: unit normal to C defined by the Frenet formula $\mathrm{d}\boldsymbol{\tau}/\mathrm{d}s = \kappa \boldsymbol{m}$; $\theta_m \equiv \boldsymbol{\theta} \,.\, \boldsymbol{m}$). Splitting the gradient of f into tangent and normal parts with respect to C, i.e.

$$\nabla f = \frac{\mathrm{d}t}{\mathrm{d}s} + (\nabla f)_\perp$$

it is readily seen that identity (9) is equivalent, *if the curve C is closed*, to

$$\frac{\mathrm{d}}{\mathrm{d}t} \int_C f \, \mathrm{d}s = \int_C \{\overset{*}{f} - f \kappa \theta_m\} \, \mathrm{d}s \tag{10}$$

where the derivative $\overset{*}{f}$ now implicitly assumes that $\theta_\tau = 0$. This simply reflects the fact that the closed curves $C + t\theta_\tau \boldsymbol{\tau}$ and C are identical up to first order in t.

In this paper, Lagrangian derivatives are defined so as to reflect the effect of geometry (i.e. crack) variations alone, with fixed load, on field variables; the prime $(\,)'$ reflects the effect of load variations with the geometry kept fixed. The total derivative of (say) the displacement field under both load and geometry variations is thus expressed as

$$\frac{\mathrm{d}\boldsymbol{u}}{\mathrm{d}t} = \overset{*}{\boldsymbol{u}} + \boldsymbol{u}'$$

The requirements (3) imply that θ must satisfy the following conditions:

$$\theta_n = 0 \quad \text{on } \Gamma \qquad \boldsymbol{\theta} \equiv 0 \quad \text{on } \partial\Omega\backslash\Gamma \tag{11}$$

In addition, one can assume without loss of generality that

$$\theta_\tau = 0 \quad \text{on } \partial\Gamma \tag{12}$$

since the closed curves $\partial\Gamma + t\theta_\tau\boldsymbol{\tau}$ and $\partial\Gamma$ are identical up to first order in t. Let Θ denote the set of all transformation velocity fields verifying (11)–(12).

3. Formulation of the rate problem for crack extension

The equilibrium solution for the current load and crack configuration has a potential energy $W = W(\bar{\boldsymbol{u}}, \bar{\boldsymbol{t}}; \Gamma)$ which, for the present context of linear elasticity and assuming the absence of body forces, is given by

$$W(\bar{\boldsymbol{u}}, \bar{\boldsymbol{t}}; \Gamma) = \frac{1}{2}\int_\Omega \boldsymbol{\sigma} : \boldsymbol{\varepsilon}\, \mathrm{d}V - \int_{S_T} \bar{\boldsymbol{t}}.\boldsymbol{u}\, \mathrm{d}S \tag{13}$$

Let $(\boldsymbol{u}_0, \boldsymbol{\varepsilon}_0, \boldsymbol{\sigma}_0)$ denote the equilibrium solution for the original boundary data $(\bar{\boldsymbol{u}}, \bar{\boldsymbol{t}})$ and in the absence of the crack, and let $(\boldsymbol{u}_1, \boldsymbol{\varepsilon}_1, \boldsymbol{\sigma}_1)$ be the elastic state associated with given tractions on the crack faces:

$$\boldsymbol{t}(\boldsymbol{x}^\pm) = \pm\boldsymbol{\sigma}_0.\boldsymbol{n} \quad (\text{on } \Gamma^\pm) \tag{14}$$

and homogeneous boundary data on S_u and S_T, so that $\boldsymbol{u} = \boldsymbol{u}_0 + \boldsymbol{u}_1$, $\boldsymbol{\varepsilon} = \boldsymbol{\varepsilon}_0 + \boldsymbol{\varepsilon}_1$, $\boldsymbol{\sigma} = \boldsymbol{\sigma}_0 + \boldsymbol{\sigma}_1$. Then, one can show that

$$W(\bar{\boldsymbol{u}}, \bar{\boldsymbol{t}}; \Gamma) = W_0(\bar{\boldsymbol{u}}, \bar{\boldsymbol{t}}) + \frac{1}{2}\int_\Gamma \bar{\boldsymbol{t}}.\boldsymbol{\phi}\, \mathrm{d}S \tag{15}$$

where $\boldsymbol{\phi} \equiv \boldsymbol{u}^+ - \boldsymbol{u}^- = \boldsymbol{u}_1^+ - \boldsymbol{u}_1^-$ is the crack opening displacement (COD) on Γ, $W_0(\bar{\boldsymbol{u}}, \bar{\boldsymbol{t}})$ is the potential energy of the state $(\boldsymbol{u}_0, \boldsymbol{\varepsilon}_0, \boldsymbol{\sigma}_0)$. Note that $W(\bar{\boldsymbol{u}}, \bar{\boldsymbol{t}}; \Gamma)$ depends on the crack configuration both explicitly and implicitly (through $\boldsymbol{\phi}$), and that W_0 is left unchanged by any crack perturbation

$$\overset{*}{W}_0(\bar{\boldsymbol{u}}, \bar{\boldsymbol{t}}) = 0 \tag{16}$$

The energy release rate $G(s)$ is mathematically defined as the kernel function associated with the domain derivative of $-W$ in any relevant domain transformation, i.e.

$$\overset{*}{W} + \int_\Gamma G\theta_\nu\, \mathrm{d}s = 0 \tag{17}$$

The crack is assumed to grow according to the Griffith criterion, which stipulates that the actual crack extension velocity $\boldsymbol{\mu}$ verify:

$$\boldsymbol{\mu} \in \Theta \quad \begin{cases} G < G_c & \mu_\nu = 0 \text{ (no extension)} \\ G = G_c & \mu_\nu \geqslant 0 \text{ (possible extension)} \end{cases} \tag{18}$$

Denote by $\Theta_c \in \Theta$ the set of extension velocity fields which satisfy the above criterion at any point of the crack edge $\partial\Gamma$. The rate problem for the current crack and load configuration consists of investigating a possible infinitesimal crack extension $\mathrm{d}\Gamma = \mu_\nu\, \mathrm{d}t$ induced by a load increment $\mathrm{d}\bar{\boldsymbol{t}} = \bar{\boldsymbol{t}}'\, \mathrm{d}t$ applied during the 'time' interval $\mathrm{d}t$.

The formulation adopted here for the rate problem is a direct adaptation of the work of Nguyen et al. [17,18]. Its main unknown is the actual crack extension velocity θ_ν, sought as a response to a given loading rate $\bar{\boldsymbol{t}}'$. Introduce the part $\partial\Gamma_c$ of the crack edge $\partial\Gamma$ on which $G = G_c$. Denote by $(\overset{\diamond}{})$ the 'material' derivative associated with the unknown velocity $\boldsymbol{\mu}$ and for *fixed* load.

The equality (17) must be maintained in the crack extension. Applying the Lagrangian derivative $(\overset{\diamond}{})$ thus gives, using identity (10):

$$\forall\, \boldsymbol{\theta} \in \Theta \quad \int_{\partial\Gamma} \theta_\nu \left[\frac{\mathrm{d}G}{\mathrm{d}t} - G\kappa\mu_m \right] \mathrm{d}s + \overset{*}{\overset{\diamond}{W}} + \overset{*}{W}' = 0 \tag{19}$$

where $\overset{*}{\overset{\diamond}{W}}$ denotes the operation of applying the Lagrangian derivative ($^\diamond$) in the velocity $\boldsymbol{\mu}$ to the first-order derivative $\overset{*}{W}$ (which depends linearly on $\boldsymbol{\theta}$) *with the additional provision that* $\overset{\diamond}{\boldsymbol{\theta}} = 0$. The latter is acceptable because $\boldsymbol{\theta}$ acts as a test function in (17): the requirement $\overset{\diamond}{\boldsymbol{\theta}} = 0$ amounts to stating that the set of test functions Θ_t associated to the perturbed crack $\Gamma + t\boldsymbol{\mu}$ is obtained from the set Θ_0 for the initial crack Γ by transport in the transformation (2).

The equality (19) holds for any $\boldsymbol{\theta} \in \Theta$, and is thus in particular true for $\boldsymbol{\theta}$ replaced by $\boldsymbol{\theta} - \boldsymbol{\mu}$ with $(\boldsymbol{\mu}, \boldsymbol{\theta}) \in \Theta_c$. Introducing the bilinear form $Q(\boldsymbol{\theta}, \boldsymbol{\mu})$:

$$Q(\boldsymbol{\theta}, \boldsymbol{\mu}) = \overset{*}{\overset{\diamond}{W}} - G_c \int_{\partial\Gamma} \mu_m \theta_\nu \kappa \, \mathrm{d}s \tag{20}$$

one obtains the following identity:

$$\forall\, \boldsymbol{\theta} \in \Theta_c \quad \int_{\partial\Gamma} \frac{\mathrm{d}G}{\mathrm{d}t} (\theta_\nu - \mu_\nu) \, \mathrm{d}S - \int_{\partial\Gamma} (G - G_c)(\theta_\nu - \mu_\nu)\mu_m \kappa \, \mathrm{d}s + Q(\boldsymbol{\theta} - \boldsymbol{\mu}, \boldsymbol{\mu}) + (\overset{\diamond}{W} - \overset{*}{W})' = 0 \tag{21}$$

Then, one notes that the Griffith criterion implies the inequality:

$$\int_{\partial\Gamma} \frac{\mathrm{d}G}{\mathrm{d}t} [\theta_\nu - \mu_\nu] \, \mathrm{d}s \leqslant 0 \quad \forall\, \boldsymbol{\theta} \in \Theta_c \tag{22}$$

which includes the cases:

$$\begin{cases} \mu_\nu \geqslant 0 & \text{if } G(s) = G_c \quad \text{and} \quad \dfrac{\mathrm{d}G}{\mathrm{d}t} = 0 \\ \mu_\nu = 0 & \text{if } G(s) < G_c \quad \text{or} \quad G(s) = G_c, \dfrac{\mathrm{d}G}{\mathrm{d}t} < 0 \end{cases}$$

and also that

$$(\forall\, \boldsymbol{\mu}, \boldsymbol{\theta} \in \Theta_c) \quad [G - G_c](\theta_\nu - \mu_\nu) \, \mathrm{d}s = 0 \tag{23}$$

Then, substitution of inequality (22) and identity (23) into Eq. (21) yields the variational inequality:

$$\text{Find } \boldsymbol{\mu} \in \Theta_c \text{ such that } (\forall\, \boldsymbol{\theta} \in \Theta_c) \quad Q(\boldsymbol{\theta} - \boldsymbol{\mu}, \boldsymbol{\mu}) + (\overset{\diamond}{W} - \overset{*}{W})' \geqslant 0 \tag{24}$$

To investigate the stability of instantaneous crack extension (i.e. the existence of a solution $\boldsymbol{\mu}$ to the variational inequality (24), ensuring its controllability by the loading evolution) and the possibility of multiple solutions for $\boldsymbol{\mu}$, the quadratic form Q defined by (20) plays a major role. It is shown in [1,16] that the instantaneous extension is stable (i.e. a solution $\boldsymbol{\mu}$ exists) if

$$Q(\boldsymbol{\theta}, \boldsymbol{\theta}) > 0 \quad \forall\, \boldsymbol{\theta} \in \Theta_c, \theta_\nu \neq \mathbf{0} \tag{25}$$

and that the solution $\boldsymbol{\mu}$ to the variational inequality (24) is unique subject to the stronger condition:

$$Q(\boldsymbol{\theta} - \boldsymbol{\mu}, \boldsymbol{\theta} - \boldsymbol{\mu}) > 0 \quad \forall\, \boldsymbol{\theta} \in \Theta_c \quad \forall\, \boldsymbol{\mu} \in \Theta_c, \theta_\nu \neq \mu_\nu \tag{26}$$

Note that, since a given instantaneous crack propagation is characterized only by the *normal extension velocity* $\mu_\nu|_\Gamma$, the uniqueness criterion refers only to the normal component μ_ν.

The most important steps in the formulation of the rate problem are thus the governing equation (17) for G and the variational inequality (24). They do not depend on the solution technique invoked for the initial elastic equilibrium problem. The practical issue now is of course how to evaluate the first- and second-order derivatives of W. The basic purpose of the present θ-integral method is to provide boundary-only expressions of the energy derivatives, thus allowing their computations in a boundary element framework.

4. General BIE-based formulation for potential energy derivatives

The symmetric Galerkin boundary integral equation (SGBIE) formulation for elastic solids with cracks governs the boundary unknowns: traction $\boldsymbol{t}$ on S_u, displacement $\boldsymbol{u}$ on S_T and COD $\boldsymbol{\phi}$ on the crack surface Γ. It takes the following general form:

$$\forall\,(\tilde{\boldsymbol{u}}, \tilde{\boldsymbol{t}}, \tilde{\boldsymbol{\phi}}) \quad \begin{cases} \mathscr{B}_{tt}(\tilde{\boldsymbol{t}}, \boldsymbol{t}) + \mathscr{B}_{tu}(\tilde{\boldsymbol{t}}, \boldsymbol{u}) + \mathscr{B}_{t\phi}(\tilde{\boldsymbol{t}}, \boldsymbol{\phi}) = \mathscr{F}_t(\tilde{\boldsymbol{t}}) \\ \mathscr{B}_{ut}(\tilde{\boldsymbol{u}}, \boldsymbol{t}) + \mathscr{B}_{uu}(\tilde{\boldsymbol{u}}, \boldsymbol{u}) + \mathscr{B}_{u\phi}(\tilde{\boldsymbol{u}}, \boldsymbol{\phi}) = \mathscr{F}_u(\tilde{\boldsymbol{u}}) \\ \mathscr{B}_{\phi t}(\tilde{\boldsymbol{\phi}}, \boldsymbol{t}) + \mathscr{B}_{\phi u}(\tilde{\boldsymbol{\phi}}, \boldsymbol{u}) + \mathscr{B}_{\phi\phi}(\tilde{\boldsymbol{\phi}}, \boldsymbol{\phi}) = \mathscr{F}_\phi(\tilde{\boldsymbol{\phi}}) \end{cases} \tag{27}$$

where the bilinear forms $\mathscr{B}_{ij}$ and linear forms $\mathscr{F}_i$ are expressed in terms of double surface integrals (see [5] or [13] for detailed expressions). In particular, using again the decomposition $\boldsymbol{u} = \boldsymbol{u}_0 + \boldsymbol{u}_1$, one can show that the governing SGBIE for the state $\boldsymbol{u}_1$, is of the form:

$$\forall\,(\tilde{\boldsymbol{u}}, \tilde{\boldsymbol{t}}, \tilde{\boldsymbol{\phi}}) \quad \begin{cases} \mathscr{B}_{tt}(\tilde{\boldsymbol{t}}, \boldsymbol{t}_1) + \mathscr{B}_{tu}(\tilde{\boldsymbol{t}}, \boldsymbol{u}_1) + \mathscr{B}_{t\phi}(\tilde{\boldsymbol{t}}, \boldsymbol{\phi}) = 0 \\ \mathscr{B}_{ut}(\tilde{\boldsymbol{u}}, \boldsymbol{t}_1) + \mathscr{B}_{uu}(\tilde{\boldsymbol{u}}, \boldsymbol{u}_1) + \mathscr{B}_{u\phi}(\tilde{\boldsymbol{u}}, \boldsymbol{\phi}) = 0 \\ \mathscr{B}_{\phi t}(\tilde{\boldsymbol{\phi}}, \boldsymbol{t}_1) + \mathscr{B}_{\phi u}(\tilde{\boldsymbol{\phi}}, \boldsymbol{u}_1) + \mathscr{B}_{\phi\phi}(\tilde{\boldsymbol{\phi}}, \boldsymbol{\phi}) = -\int_\Gamma \tilde{\boldsymbol{\phi}}\,.\,\bar{\boldsymbol{t}}\,\mathrm{d}S \end{cases} \tag{28}$$

The formulations (27), (28) are symmetric, and lead after BEM discretization to symmetric linear systems of equations for the unknowns boundary DOFs. It has been shown in [5] that the SGBIE formulation (27) is nothing else than the stationarity equation for the potential energy constrained by the Dirichlet boundary data, restricted to trial functions (i.e. displacement variations) solving the homogeneous Navier (i.e. elastic equilibrium) equation.

To formulate the derivatives of the potential energy W given by (15), it is advantageous to introduce the Lagrangian $\mathscr{L}$:

$$\mathscr{L}(\boldsymbol{u}_1, \tilde{\boldsymbol{u}}, \bar{\boldsymbol{u}}, \Gamma) = W_0(\bar{\boldsymbol{u}}) + \frac{1}{2}\int_\Gamma \bar{\boldsymbol{t}}\,.\,\boldsymbol{\phi}\,\mathrm{d}S + \mathscr{B}(\boldsymbol{u}_1, \tilde{\boldsymbol{u}}) + \int_\Gamma \tilde{\boldsymbol{\phi}}\,.\,\bar{\boldsymbol{t}}\,\mathrm{d}S \tag{29}$$

where $\boldsymbol{u}$, $\tilde{\boldsymbol{u}}$, $\bar{\boldsymbol{u}}$, $\mathscr{B}$ are compact notations for the set of unknowns, trial functions, external boundary data and bilinear forms. The underlying idea, very commonly used in optimal control, is to treat formally the variables $(\boldsymbol{u}_1, \Gamma)$ as independent and incorporate the state equation (28) as a constraint term.

4.1. First-order domain derivatives of W

Consider the application of Lagrangian differentiation to (28), assuming that (i) $(\tilde{\boldsymbol{u}})^* = \boldsymbol{0}$ (i.e. the space of test functions is convected in the domain transformation) and (ii) the loading is kept constant, i.e.

$$\overset{*}{\bar{\boldsymbol{t}}} = \boldsymbol{\nabla}\bar{\boldsymbol{t}}\,.\,\boldsymbol{\theta} \quad \text{on } \Gamma \tag{30}$$

One first obtains (note that $\overset{*}{\boldsymbol{u}}_1 = \overset{*}{\boldsymbol{u}}$):

$$\overset{*}{\mathscr{B}}(\boldsymbol{u}_1, \tilde{\boldsymbol{u}}) = \mathscr{B}(\overset{*}{\boldsymbol{u}}, \tilde{\boldsymbol{u}}) + \mathscr{B}^1(\boldsymbol{u}_1, \tilde{\boldsymbol{u}}; \boldsymbol{\theta}) \tag{31}$$

The above equalities define $\mathscr{B}^1$ (which depends linearly on $\boldsymbol{\theta}$). Besides, one has

$$\begin{aligned} \frac{\mathrm{d}}{\mathrm{d}t}\int_\Gamma \boldsymbol{\phi}\,.\,\bar{\boldsymbol{t}}\,\mathrm{d}S &= \int_\Gamma \overset{*}{\boldsymbol{\phi}}\,.\,\bar{\boldsymbol{t}}\,\mathrm{d}S + \int_\Gamma \boldsymbol{\phi}\,.\,(\boldsymbol{\nabla}\bar{\boldsymbol{t}}\,.\,\boldsymbol{\theta} + \bar{\boldsymbol{t}}\,\mathrm{div}_S\boldsymbol{\theta})\,\mathrm{d}S \\ &= \int_\Gamma \overset{*}{\boldsymbol{\phi}}\,.\,\bar{\boldsymbol{t}}\,\mathrm{d}S - \int_\Gamma (\boldsymbol{\nabla}\boldsymbol{\phi}\,.\,\boldsymbol{\theta})\,.\,\bar{\boldsymbol{t}}\,\mathrm{d}S \end{aligned} \tag{32}$$

where the differentiation $\mathrm{d}/\mathrm{d}t$ is performed for constant loading (the latter equality results from an integration by parts). The derivative $\overset{*}{\mathscr{L}}$ then takes the form (using the fact that $\overset{*}{W}_0 = 0$):

$$\overset{*}{\mathscr{L}} = \frac{1}{2}\int_\Gamma \overset{*}{\phi}.\bar{t}\,\mathrm{d}S + \mathscr{B}(\tilde{u},\overset{*}{\tilde{u}}) - \frac{1}{2}\int_\Gamma (\nabla\phi.\theta).\bar{t}\,\mathrm{d}S - \int_\Gamma (\nabla\tilde{\phi}.\theta).\bar{t}\,\mathrm{d}S + \mathscr{B}^1(\tilde{u},u_1;\theta) \tag{33}$$

Now, one notices that the particular choice $\tilde{u} = u_1/2$ for the multiplier $\tilde{u}$ ensures that

$$\frac{1}{2}\int_\Gamma \overset{*}{\phi}.\bar{t}\,\mathrm{d}S + \mathscr{B}(\tilde{u},\overset{*}{\tilde{u}}) = 0 \quad (\forall\,\overset{*}{\tilde{u}} \in \mathscr{V})$$

by virtue of the SGBIE formulation (28) and using the symmetry of the bilinear form $\mathscr{B}$ (this selection of $\tilde{u}$ is a particular instance of the *adjoint state* concept). This results in the following expression for $\overset{*}{W}$, which is linear in θ:

$$\overset{*}{W} = \frac{1}{2}\,\mathscr{B}^1(u_1,u_1;\theta) - \int_\Gamma (\nabla\phi.\theta).\bar{t}\,\mathrm{d}S \tag{34}$$

It can be shown that $\overset{*}{W}$ depends on θ only through the normal extension velocity on the crack front $\theta_\nu|_{\partial\Gamma}$; in other words, if $\theta^{(1)}$, $\theta^{(2)}$ are such that $\theta_\nu^{(1)} = \theta_\nu^{(2)}$, then $W_{,\Gamma}(\bar{t},\Gamma).\theta^{(2)} = W_{,\Gamma}(\bar{t},\Gamma).\theta^{(2)}$. Hence, the result (34) is in practice applied to extension velocity fields θ defined as arbitrary extensions over Γ of given normal extension velocities θ_ν over $\partial\Gamma$, see Section 6.

4.2. Second-order domain derivatives of W

The Lagrangian derivative of $\mathscr{B}^1$ takes the form:

$$\overset{\diamond}{\mathscr{B}}{}^1(u,\tilde{u};\theta) = \mathscr{B}^1(\overset{\diamond}{u},\tilde{u};\theta) + \mathscr{B}^2(u,\tilde{u};\theta,\mu) \tag{35}$$

which defines $\mathscr{B}^2$, a bilinear form in (θ,μ). Moreover, from (5), (6), one has

$$\frac{\mathrm{d}}{\mathrm{d}t}\int_\Gamma (\nabla\phi.\theta).\bar{t}\,\mathrm{s}S = \int_\Gamma (\nabla\overset{\diamond}{\phi}.\theta).\bar{t}\,\mathrm{d}S + \int_\Gamma \{(\nabla\phi.\theta).(\nabla\bar{t}.\mu + \bar{t}\,\mathrm{div}_S\,\mu) - (\nabla\phi.\nabla\mu.\theta).\bar{t}\}\,\mathrm{d}S \tag{36}$$

where the Lagrangian differentiation $\mathrm{d}/\mathrm{d}t$ is taken for constant loading and in the velocity field μ. Then, one can express the second-order derivative $\overset{*\diamond}{W}$ from (34) as

$$\begin{aligned}\overset{*\diamond}{W} &= \mathscr{B}^1(u,\overset{\diamond}{u};\theta) + \frac{1}{2}\,\mathscr{B}^2(u,u;\theta,\mu) - \int_\Gamma (\nabla\overset{\diamond}{\phi}.\theta).\bar{t}\,\mathrm{d}S \\ &\quad - \int_\Gamma \{(\nabla\phi.\theta).(\nabla\bar{t}.\mu + \bar{t}\,\mathrm{div}_S\,\mu) - (\nabla\phi.\nabla\mu.\theta).\bar{t}\}\,\mathrm{d}S\end{aligned} \tag{37}$$

To evaluate $\overset{*\diamond}{W}$, one thus needs the first-order derivatives $\overset{\diamond}{u}$ of the elastic state. A governing equation for $\overset{*}{u}$ is obtained by taking the Lagrangian derivative (*) of the SGBIE formulation (28), resulting in

$$(\forall\,\tilde{u}) \quad \mathscr{B}(\tilde{u},\overset{*}{\tilde{u}}) = \int_\Gamma (\nabla\tilde{\phi}.\theta).\bar{t}\,\mathrm{d}S - \mathscr{B}^1(\tilde{u},u;\theta) \tag{38}$$

Choosing $\tilde{u} = \overset{\diamond}{u}$ in (38) and substituting the corresponding equation into (37) yields the result:

$$\overset{*\diamond}{W} = \frac{1}{2}\,\mathscr{B}^2(u,u;\theta,\mu) - \mathscr{B}(\overset{*}{u},\overset{\diamond}{u}) - \int_\Gamma \{(\nabla\phi.\theta).(\nabla\bar{t}.\mu + \bar{t}\,\mathrm{div}_S\,\mu) - (\nabla\phi.\nabla\mu.\theta).\bar{t}\}\,\mathrm{d}S \tag{39}$$

4.3. Second-order mixed domain-load derivatives of W

Eq. (34) gives

$$\overset{*}{W}' = \mathscr{B}^1(u_1,u_1';\theta) - \int_\Gamma \{(\nabla\phi'.\theta).\bar{t} + (\nabla\phi.\theta).\bar{t}'\}\,\mathrm{d}S \tag{40}$$

Then, the differentiation in a load increment of (28) yields (with $\tilde{u} = \overset{*}{u}$):

$$\mathscr{B}(\boldsymbol{u}'_1, \overset{*}{\boldsymbol{u}}) = -\int_\Gamma \overset{*}{\boldsymbol{\phi}} . \bar{\boldsymbol{t}}' \, \mathrm{d}S$$

while substituting $\tilde{\boldsymbol{u}} = \boldsymbol{u}'_1$ into the derivative SGBIE (38) gives

$$\mathscr{B}(\overset{*}{\tilde{\boldsymbol{u}}}, \boldsymbol{u}'_1) = \int_\Gamma (\nabla \boldsymbol{\phi}' . \boldsymbol{\theta}) . \bar{\boldsymbol{t}} \, \mathrm{d}S - \mathscr{B}^1(\boldsymbol{u}_1, \boldsymbol{u}'_1; \boldsymbol{\theta})$$

Substituting the last two relations into (40) results in

$$\overset{*}{W}' = \int_\Gamma (\overset{*}{\boldsymbol{\phi}} - \nabla \boldsymbol{\phi} . \boldsymbol{\theta}) . \bar{\boldsymbol{t}}' \, \mathrm{d}S \tag{41}$$

In the above result, $\bar{\boldsymbol{t}}'$ is evaluated from the derivative of the uncracked elastic state $\boldsymbol{u}_0$ in the load increment:

$$\bar{\boldsymbol{t}}' = \boldsymbol{\sigma}(\boldsymbol{u}'_0) . \boldsymbol{n} \quad \text{on } \Gamma$$

4.4. Formulation of the rate problem

The foregoing development shows in general terms how the derivatives $\overset{*}{W}$, $\overset{*\diamond}{W}$, $\overset{*}{W}'$ are set up from an initial SGBIE formulation. To actually apply this strategy one must establish explicit expressions for $\mathscr{B}^1$, $\mathscr{B}^2$.

This task is carried out in the next section for cracks of arbitrary shape embedded in an infinite medium, for which numerical examples will be presented later. Bounded elastic solids with cracks can be addressed the same way, resulting in formulas that are longer but conceptually identical.

5. Derivatives of potential energy: cracks in unbounded media

5.1. Galerkin BIE formulation

The Galerkin BIE formulation for a (possibly non-planar) crack Γ of arbitrary shape in an infinite isotropic medium $\Omega = \mathbb{R}^3$ (Poisson ratio ν, shear modulus μ), formulated by Nedelec [15], is recalled in this section for the reader's convenience. The states defined by $\boldsymbol{u}_0$ and $\boldsymbol{u}_1$ here correspond to loadings applied respectively: (i) at infinity; and (ii) symmetrically on the crack faces:

$$\boldsymbol{t}_1(\boldsymbol{x}^+) = +\bar{\boldsymbol{t}}, \qquad \boldsymbol{t}_1(\boldsymbol{x}^-) = -\bar{\boldsymbol{t}} \tag{42}$$

It is well known that any displacement field $\boldsymbol{u}$ solution to the field (Navier) equations for elastic equilibrium admits an integral representation in terms of the crack opening displacement (COD) $\boldsymbol{\phi}(\boldsymbol{y}) \equiv \boldsymbol{u}^+(\boldsymbol{y}) - \boldsymbol{u}^-(\boldsymbol{y})$ (see e.g. [3,7]):

$$u_i(z) = \int_\Gamma \Sigma'_{k\ell}(\boldsymbol{y} - \boldsymbol{z}) n_\ell(\boldsymbol{y}) \phi_k(\boldsymbol{y}) \, \mathrm{d}S_y \quad (\boldsymbol{z} \notin \Gamma) \tag{43}$$

where $\Sigma'_{k\ell}$ $(1 \leqslant i, k, \ell \leqslant 3)$ is the $k\ell$-component of the fundamental Kelvin stress tensor, i.e. the elastic stress state generated at the field point $\boldsymbol{y}$ by a unit point force applied at $\boldsymbol{z}$ along the i-direction.

One notices that the given tractions $\pm\bar{\boldsymbol{t}}$ do not appear explicitly in the previous expression. It is thus necessary to formulate an integral representation for the stress tensor $\boldsymbol{\sigma}$. The latter is associated with $\boldsymbol{u}$ through Hooke's law:

$$\sigma_{ij} = C_{ijab} u_{a,b} \qquad C_{ijab} = \mu\left(\frac{2\nu}{1-2\nu}\delta_{ij}\delta_{ab} + \delta_{ia}\delta_{jb} + \delta_{ja}\delta_{ib}\right) \tag{44}$$

so that the integral representation formula for $\boldsymbol{\sigma}$ reads

$$\sigma_{ij}(\boldsymbol{x}) = C_{ijab} \int_\Gamma \frac{\partial}{\partial x_b} \Sigma^a_{k\ell}(\boldsymbol{y} - \boldsymbol{x}) n_\ell(\boldsymbol{y}) \phi_k(\boldsymbol{y}) \, \mathrm{d}S_y \tag{45}$$

The Galerkin BIE formulation basically follows a weighted-residual approach, i.e. consists of taking the inner

product of (45) with $\tilde{\phi}_i(\boldsymbol{x})n_j(\boldsymbol{x})$, where $\tilde{\boldsymbol{\phi}}(\boldsymbol{x})$ is a test function, and integrating the result over Γ with respect to the observation point $\boldsymbol{x}$. However, due to the $|\boldsymbol{y}-\boldsymbol{z}|^{-3}$ hypersingular behavior of $\boldsymbol{\Sigma}'$, a regularization procedure is needed. To this purpose, following Sirtori et al. [23], an auxiliary surface $\tilde{\Gamma}$ close to, but not intersecting, Γ is defined by means of a one-to-one correspondence, e.g.

$$\boldsymbol{x} \in \Gamma \to \boldsymbol{z} = \boldsymbol{x} + \eta \boldsymbol{n}(\boldsymbol{x}) \in \tilde{\Gamma} \quad \text{for } \eta > 0 \text{ sufficiently small}$$

The weighted residual approach is then sought as the limiting case when $\eta \to 0$ in

$$\int_{\tilde{\Gamma}} \tilde{\phi}_i(\boldsymbol{z}) n_j(\boldsymbol{z}) \sigma_{ij}(\boldsymbol{z}) \, \mathrm{d}S_z = C_{ijab} \int_{\tilde{\Gamma}} \int_{\Gamma} n_j(\boldsymbol{z}) \tilde{\phi}_i(\boldsymbol{z}) \frac{\partial}{\partial x_b} \Sigma^a_{k\ell}(\boldsymbol{y}-\boldsymbol{z}) n_\ell(\boldsymbol{y}) \phi_k(\boldsymbol{y}) \, \mathrm{d}S_y \, \mathrm{d}S_z \tag{46}$$

Introduce the fourth-order tensor $\boldsymbol{B}(\boldsymbol{y}-\boldsymbol{z})$ defined by [15,19]

$$B_{ikqs}(\boldsymbol{y}-\boldsymbol{z}) = \frac{\mu}{8\pi} \left[\frac{2\nu}{1-\nu} \delta_{pq}\delta_{rs} + \delta_{pr}\delta_{qs} + \delta_{ps}\delta_{qr} \right] e_{iep} e_{kgr} \frac{\partial^2 r}{\partial x_e \, \partial y_g} \tag{47}$$

$\boldsymbol{B}(\boldsymbol{y}-\boldsymbol{z})$ has a weak r^{-1} singularity and verifies

$$C_{ijab} \frac{\partial}{\partial x_b} \Sigma^a_{k\ell}(\boldsymbol{y}-\boldsymbol{z}) = e_{jfq} e_{lhs} B_{ikqs,fh}(\boldsymbol{y}-\boldsymbol{z}) \quad (\boldsymbol{z} \neq \boldsymbol{y}) \tag{48}$$

Thanks to this fundamental property, a double application (once with respect to each integration variable $\boldsymbol{z}$ and $\boldsymbol{y}$) of the Stokes formula:

$$\int_{\Gamma} e_{abc} n_a f_{,b} \, \mathrm{d}S_y = \int_{\partial\Gamma} f \tau_c \, \mathrm{d}s_y \tag{49}$$

allows to recast (46) into the following equivalent form:

$$\int_{\tilde{\Gamma}} \int_{\Gamma} \tilde{\phi}_i(\boldsymbol{z}) \sigma_{ij}(\boldsymbol{z}) n_j(\boldsymbol{z}) \, \mathrm{d}S_x = \int_{\tilde{\Gamma}} \int_{\Gamma} R_q \tilde{\phi}_i(\boldsymbol{z}) B_{ikqs}(\boldsymbol{y}-\boldsymbol{z}) R_s \phi_k(\boldsymbol{y}) \, \mathrm{d}S_y \, \mathrm{d}S_z \tag{50}$$

The differential operator $R_a f$, defined by

$$R_a f = e_{bca} n_b f_{,c} \tag{51}$$

involves tangential derivatives of f only: its inner product by n_a vanishes due to the well-known properties of the permutation symbol e_{abc}.

Since $B_{ikqs}(\boldsymbol{y}-\boldsymbol{z})$ is weakly singular, the inner integral (w.r.t. $\boldsymbol{y}$) is convergent and, as a function of $\boldsymbol{z}$, continuous everywhere (and in particular across Γ). Hence, the limiting form of (50) for $\eta \to 0$, i.e. $\boldsymbol{z} \in \tilde{\Gamma} \to \boldsymbol{x} \in \Gamma$, follows at once.

As a result, the Galerkin BIE formulation for the crack problem is [15]

$$\text{find } \boldsymbol{\phi} \in \mathcal{V} \quad \mathcal{B}(\boldsymbol{\phi}, \tilde{\boldsymbol{\phi}}) = -\int_{\Gamma} \tilde{\boldsymbol{\phi}} \cdot \bar{\boldsymbol{t}} \, \mathrm{d}S \quad (\forall \, \tilde{\boldsymbol{\phi}} \in \mathcal{V}) \tag{52}$$

where the bilinear form $\mathcal{B}(\boldsymbol{\phi}, \tilde{\boldsymbol{\phi}})$ is given by

$$\mathcal{B}(\boldsymbol{\phi}, \tilde{\boldsymbol{\phi}}) = \int_{\Gamma} \int_{\Gamma} R_q \tilde{\phi}_i(\boldsymbol{x}) B_{ikqs}(\boldsymbol{y}-\boldsymbol{x}) R_s \phi_k(\boldsymbol{y}) \, \mathrm{d}S_y \, \mathrm{d}S_x \tag{53}$$

The function space $\mathcal{V}$ is

$$\mathcal{V} = \{ \tilde{\boldsymbol{\phi}} : \Gamma \to \mathbb{R}^3, \, \tilde{\boldsymbol{\phi}}|_{\partial\Gamma} = \boldsymbol{0}, \, \mathcal{B}(\tilde{\boldsymbol{\phi}}, \tilde{\boldsymbol{\phi}}) < \infty \} \tag{54}$$

5.1.1. Other cases of applicability

In addition to the isolated crack configuration, the Galerkin BIE formulation (52) also covers the following situations:

(1) Multiple cracks in an unbounded elastic medium (the surface Γ is not required to be connected);

(2) A bounded elastic body B with external ∂B containing internal cracks and with tractions prescribed over

∂B (formulation (52) for $\Gamma = \partial B \cup \Gamma'$, where Γ' are the internal cracks). In this case, $\boldsymbol{\phi}$ on ∂B is the density of a double-layer potential, not the displacement physically experienced by the body B.

5.2. Derivatives of potential energy

Explicit expressions for $\mathscr{B}^1$, $\mathscr{B}^2$ are now established through two successive applications of Lagrangian differentiation to the Galerkin BIE formulation (52), under the assumption (30), i.e for a fixed loading. It is important to note again that the space $\mathscr{V}_t$ of test functions associated to the perturbed crack $\Gamma_t = \boldsymbol{\Phi}(\Gamma, t)$ can be put in one-to-one correspondence with the space $\mathscr{V}$ of test functions associated to the original crack Γ through:

$$\tilde{\boldsymbol{\phi}} \in \mathscr{V} \to \tilde{\boldsymbol{\phi}}_t(\boldsymbol{x}) = \tilde{\boldsymbol{\phi}}(\boldsymbol{\Phi}(\boldsymbol{x}, t)) \in \mathscr{V}_t$$

which is such that

$$\frac{\mathrm{d}}{\mathrm{d}t}\,\tilde{\boldsymbol{\phi}}_t(\boldsymbol{x})\big|_{t=0} = \mathbf{0} \quad \text{i.e.} \quad \overset{*}{\tilde{\boldsymbol{\phi}}}(\boldsymbol{x}) = \mathbf{0} \tag{55}$$

Hence, one can assume $\overset{*}{\tilde{\boldsymbol{\phi}}} = \mathbf{0}$ without loss of generality. In accordance with these provisions, the derivative of the bilinear form $\mathscr{B}(\boldsymbol{\phi}, \tilde{\boldsymbol{\phi}})$ in a crack extension is given by

$$\overset{*}{\mathscr{B}}(\boldsymbol{\phi}, \tilde{\boldsymbol{\phi}}) = \mathscr{B}(\overset{*}{\boldsymbol{\phi}}, \tilde{\boldsymbol{\phi}}) + \mathscr{B}^1(\boldsymbol{\phi}, \tilde{\boldsymbol{\phi}}; \boldsymbol{\theta}) \tag{56}$$

where the new bilinear form $\mathscr{B}^1(\boldsymbol{\phi}, \tilde{\boldsymbol{\phi}}; \boldsymbol{\theta})$ is expressed in terms of a new kernel function $B^1_{ikqs}(\boldsymbol{x}, \boldsymbol{y}; \boldsymbol{\theta})$ which depends linearly on $\boldsymbol{\theta}$:

$$\begin{aligned} &\mathscr{B}^1(\boldsymbol{\phi}, \tilde{\boldsymbol{\phi}}; \boldsymbol{\theta}) = \int_\Gamma \int_\Gamma R_q \tilde{\phi}_i(\boldsymbol{x}) B^1_{ikqs}(\boldsymbol{x}, \boldsymbol{y}; \boldsymbol{\theta}) R_s \phi_k(\boldsymbol{y})\, \mathrm{d}S_x\, \mathrm{d}S_y \\ &B^1_{ikqs}(\boldsymbol{x}, \boldsymbol{y}; \boldsymbol{\theta}) = [\theta_a(\boldsymbol{y}) - \theta_a(\boldsymbol{x})] B_{ikqs,a}(\boldsymbol{y} - \boldsymbol{x}) + B_{ikqa}(\boldsymbol{y} - \boldsymbol{x}) \theta_{a,s}(\boldsymbol{y}) + B_{ikas}(\boldsymbol{y} - \boldsymbol{x}) \theta_{a,q}(\boldsymbol{x}) \end{aligned} \tag{57}$$

The above result stems from an application of formula (8) to (53). Use has been made of the following identity:

$$(R_a f)^* = \theta_{a,q} R_q f \tag{58}$$

Next, applying formula (8) (with θ replaced by $\boldsymbol{\mu}$) to (57) yields the derivative of the quadratic form $\mathscr{B}^1(\boldsymbol{\phi}, \boldsymbol{\phi}; \boldsymbol{\theta})$ in the extension velocity $\boldsymbol{\mu}$:

$$\overset{\diamond}{\mathscr{B}}_1(\boldsymbol{\phi}, \boldsymbol{\phi}; \theta) = 2\mathscr{B}^1(\boldsymbol{\phi}, \overset{\diamond}{\boldsymbol{\phi}}; \boldsymbol{\theta}) + \mathscr{B}^2(\boldsymbol{\phi}, \boldsymbol{\phi}; \boldsymbol{\theta}, \boldsymbol{\mu}) \tag{59}$$

where the new bilinear form $\mathscr{B}^2(\boldsymbol{\phi}, \tilde{\boldsymbol{\phi}}; \boldsymbol{\theta}, \boldsymbol{\mu})$ is expressed in terms of a new kernel function $B^2_{ikqs}(\boldsymbol{x}, \boldsymbol{y}; \boldsymbol{\theta}, \boldsymbol{\mu})$ which is bilinear in $(\boldsymbol{\theta}, \boldsymbol{\mu})$:

$$\mathscr{B}^2(\boldsymbol{\phi}, \boldsymbol{\phi}; \boldsymbol{\theta}, \boldsymbol{\mu}) = \int_\Gamma \int_\Gamma R_q \tilde{\phi}_i(\boldsymbol{x}) R_s \phi_k(\boldsymbol{y}) B^2_{ikqs}(\boldsymbol{x}, \boldsymbol{y}; \boldsymbol{\theta}, \boldsymbol{\mu})\, \mathrm{d}S_x\, \mathrm{d}S_y \tag{60}$$

where (using the fact that the set Θ_t can be defined so as to have $\overset{\diamond}{\boldsymbol{\theta}} = \mathbf{0}$)

$$\begin{aligned} C_{ikqs}(\boldsymbol{x}, \boldsymbol{y}; \boldsymbol{\theta}, \boldsymbol{\mu}) = {} & [\theta_a(\boldsymbol{y}) - \theta_a(\boldsymbol{x})][\mu_b(\boldsymbol{y}) - \mu_b(\boldsymbol{x})] B_{ikqs,ab}(\boldsymbol{y} - \boldsymbol{x}) \\ & + [\mu_b(\boldsymbol{y}) - \mu_b(\boldsymbol{x})]\{\theta_{a,s}(\boldsymbol{y}) B_{ikqa,b}(\boldsymbol{y} - \boldsymbol{x}) + \theta_{a,q}(\boldsymbol{y}) B_{ikas,b}(\boldsymbol{y} - \boldsymbol{x})\} \\ & + [\theta_b(\boldsymbol{y}) - \theta_b(\boldsymbol{x})]\{\mu_{a,s}(\boldsymbol{y}) B_{ikqa,b}(\boldsymbol{y} - \boldsymbol{x}) + \mu_{a,q}(\boldsymbol{y}) B_{ikas,b}(\boldsymbol{y} - \boldsymbol{x})\} \\ & + B_{ikab}(\boldsymbol{y} - \boldsymbol{x})\{\mu_{a,s}(\boldsymbol{y}) \theta_{b,q}(\boldsymbol{x}) + \mu_{a,q}(\boldsymbol{x}) \theta_{b,s}(\boldsymbol{y})\} \end{aligned}$$

Eqs. (57) and (60), which express the terms $\mathscr{B}^1$, $\mathscr{B}^2$ in boundary-only form, constitute the main results of this section.

5.2.1. Symmetry of $\overset{*}{W}^{\diamond}$ *in* $(\boldsymbol{\theta}, \boldsymbol{\mu})$

It is important to remark that $\overset{*}{W}^{\diamond}$ given by (39) is symmetric with respect to $(\boldsymbol{\theta}, \boldsymbol{\mu})$. This property follows from the following identity, established in Appendix A.2 using repeated integrations by parts:

$$\begin{aligned}
&\int_\Gamma \{(\nabla\boldsymbol{\phi}\,.\,\boldsymbol{\theta})\,.\,(\nabla\bar{\boldsymbol{t}}\,.\,\boldsymbol{\mu} + \bar{\boldsymbol{t}}\,\mathrm{div}_S\,\boldsymbol{\mu}) - (\nabla\boldsymbol{\phi}\,.\,\nabla\boldsymbol{\mu}\,.\,\boldsymbol{\theta})\,.\,\bar{\boldsymbol{t}}\}\,\mathrm{d}S \\
&\quad = \int_\Gamma (\nabla\boldsymbol{\theta} : \nabla\boldsymbol{\mu} + K(\boldsymbol{\theta}\,.\,\boldsymbol{\mu}) - \mathrm{div}_S\,\boldsymbol{\theta}\,\mathrm{div}_S\,\boldsymbol{\mu})(\boldsymbol{\phi}\,.\,\bar{\boldsymbol{t}})\,\mathrm{d}S \\
&\qquad + \frac{1}{2}\int_\Gamma \{(\nabla\boldsymbol{\phi}\,.\,\boldsymbol{\theta})\,.\,(\nabla\bar{\boldsymbol{t}}\,.\,\boldsymbol{\mu}) + (\nabla\boldsymbol{\phi}\,.\,\boldsymbol{\mu})\,.\,(\nabla\bar{\boldsymbol{t}}\,.\,\boldsymbol{\theta})\}\,\mathrm{d}S \\
&\qquad + \frac{1}{2}\int_\Gamma \boldsymbol{\phi}\,.\,\nabla\bar{\boldsymbol{t}}\,.\,(\nabla\boldsymbol{\theta}\,.\,\boldsymbol{\mu} + \nabla\boldsymbol{\mu}\,.\,\boldsymbol{\theta} - \boldsymbol{\theta}\,\mathrm{div}_S\,\boldsymbol{\mu} - \boldsymbol{\mu}\,\mathrm{div}_S\,\boldsymbol{\theta})\,\mathrm{d}S
\end{aligned} \tag{61}$$

Moreover, the symmetry of $\mathscr{B}(\boldsymbol{\phi}, \tilde{\boldsymbol{\phi}})$ in $(\boldsymbol{\phi}, \tilde{\boldsymbol{\phi}})$ implies that of $\mathscr{B}(\overset{*}{\boldsymbol{\phi}}^{\diamond}, \boldsymbol{\phi})$ in $(\boldsymbol{\theta}, \boldsymbol{\mu})$. Finally, the symmetry of $\mathscr{B}^2(\boldsymbol{\phi}, \boldsymbol{\phi}; \boldsymbol{\theta}, \boldsymbol{\mu})$ in $(\boldsymbol{\theta}, \boldsymbol{\mu})$ is apparent in Eq. (60).

5.2.2. Formulation of the instantaneous crack extension problem

It is achieved by direct substitution of formulas (34) into (17), using expression (57) for $\mathscr{B}^1$, and (39), (41) into the variational inequality (24) and the definition (20), using expression (60) for $\mathscr{B}^2$.

5.3. Special case of a planar crack

The numerical examples to be presented in Section 7 concern planar cracks. Accordingly, Eqs. (53), (57), (60) are now given in a more explicit form for planar cracks. The surface Γ lies in the $(\boldsymbol{e}_1, \boldsymbol{e}_2)$ coordinate plane, the crack front $\partial\Gamma$ being a closed planar curve; the unit normal to Γ is taken as $\boldsymbol{n} = +\boldsymbol{e}_3$.

5.3.1. Expression of $\mathscr{B}(\phi, \tilde{\phi})$

One has, as shown in Appendix A.3:

$$\begin{aligned}
\mathscr{B}(\boldsymbol{\phi}, \tilde{\boldsymbol{\phi}}) = {} & \frac{\mu}{4\pi(1-\nu)}\int_\Gamma\int_\Gamma \tilde{\phi}_{3,h}(\boldsymbol{x})\phi_{3,h}(\boldsymbol{y})\,\frac{1}{r}\,\mathrm{d}S_x\,\mathrm{d}S_y \\
& + \frac{\mu}{4\pi}\int_\Gamma\int_\Gamma \left[\tilde{\phi}_{i,h}(\boldsymbol{x})\phi_{i,h}(\boldsymbol{y}) + \frac{\nu}{1-\nu}\,\tilde{\phi}_{i,i}(\boldsymbol{x})\phi_{k,k}(\boldsymbol{y})\right]\frac{1}{r}\,\mathrm{d}S_x\,\mathrm{d}S_y
\end{aligned} \tag{62}$$

(with $i, h, k = 1, 2$). The above expression emphasizes the well-known uncoupling between mode I (opening, i.e. $(\phi_3, \tilde{\phi}_3)$) and modes II–III (sliding, i.e. $(\phi_i, \tilde{\phi}_i)$, $i = 1, 2$). The governing Galerkin BIE formulation for the COD in mode I thus reads

$$\forall\,\tilde{\phi} \in \mathscr{V} \quad \frac{\mu}{4\pi(1-\nu)}\int_\Gamma\int_\Gamma \tilde{\phi}_{,h}(\boldsymbol{x})\phi_{,h}(\boldsymbol{y})\,\frac{1}{r}\,\mathrm{d}S_x\,\mathrm{d}S_y = \int_\Gamma \tilde{\phi}(\boldsymbol{x})\bar{t}(\boldsymbol{x})\,\mathrm{d}S_x \tag{63}$$

(with $\phi \equiv \phi_3$, $\tilde{\phi} \equiv \tilde{\phi}_3$, $\bar{t} \equiv \bar{t}_3$). For modes II–III, one has

$$\forall\,\tilde{\phi} \in \mathscr{V} \quad \frac{\mu}{4\pi}\int_\Gamma\int_\Gamma \left[\tilde{\phi}_{i,h}(\boldsymbol{x})\phi_{i,h}(\boldsymbol{y}) + \frac{\nu}{1-\nu}\,\tilde{\phi}_{i,i}(\boldsymbol{x})\phi_{k,k}(\boldsymbol{y})\right]\frac{1}{r}\,\mathrm{d}S_x\,\mathrm{d}S_y = \int_\Gamma \tilde{\phi}_i(\boldsymbol{x})\bar{t}_i(\boldsymbol{x})\,\mathrm{d}S_x \tag{64}$$

5.3.2. Expression of $\mathscr{B}^1(\boldsymbol{\phi}, \tilde{\boldsymbol{\phi}}; \boldsymbol{\theta})$

It stems from either a direct application of formula (6) to (63)–(64) or a specialization to planar cracks of Eq. (57). As a result, one has

$$\mathcal{B}^1(\boldsymbol{\phi}, \tilde{\boldsymbol{\phi}}; \boldsymbol{\theta}) = \frac{\mu}{4\pi} \chi \int_\Gamma \int_\Gamma \left[(A\delta_{ik} - B_{ik})\theta_{i,k}(\boldsymbol{x}) \frac{1}{r} + \frac{A}{2} [\theta_h(\boldsymbol{y}) - \theta_h(\boldsymbol{x})] \left(\frac{1}{r}\right)_{,h} \right] \mathrm{d}S_x \, \mathrm{d}S_y \tag{65}$$

where $\chi = 1/(1-\nu)$ for mode I and $\chi = 1$ for modes II–III, and

$$B_{ik} = \tilde{\phi}_{,i}(\boldsymbol{x})\phi_{,k}(\boldsymbol{y}) + \phi_{,i}(\boldsymbol{x})\tilde{\phi}_{,k}(\boldsymbol{y}) \quad \text{(mode I)}$$

$$= \tilde{\phi}_{h,i}(\boldsymbol{x})\phi_{h,k}(\boldsymbol{y}) + \phi_{h,i}(\boldsymbol{x})\tilde{\phi}_{h,k}(\boldsymbol{y}) + \frac{\nu}{1-\nu}(\tilde{\phi}_{k,i}(\boldsymbol{x})\phi_{h,h}(\boldsymbol{y}) + \phi_{k,i}(\boldsymbol{x})\tilde{\phi}_{h,h}(\boldsymbol{y})) \quad \text{(mode II–III)}$$

$$A = B_{ii}$$

5.3.3. Expression of $\mathcal{B}^2(\boldsymbol{\phi}, \tilde{\boldsymbol{\phi}}; \boldsymbol{\theta}, \boldsymbol{\mu})$

It stems from either a direct application of formula (8) to (65) or a specialization to planar cracks of (60):

$$\begin{aligned}\mathcal{B}^2(\boldsymbol{\phi}, \boldsymbol{\phi}; \boldsymbol{\theta}, \boldsymbol{\mu}) = \frac{\mu}{4\pi} x \int_\Gamma \int_\Gamma \Big\{ & \frac{A}{2} [\theta_h(\boldsymbol{y}) - \theta_h(\boldsymbol{x})][\mu_k(\boldsymbol{y}) - \mu_k(\boldsymbol{x})] \left(\frac{1}{r}\right)_{,hk} \\ & + (A\delta_{ik} - B_{ik})(\theta_{i,k}(\boldsymbol{x})[\mu_h(\boldsymbol{y}) - \mu_h(\boldsymbol{x})] + \mu_{i,k}(\boldsymbol{x})[\theta_h(\boldsymbol{y}) - \theta_h(\boldsymbol{x})]) \left(\frac{1}{r}\right)_{,h} \\ & + \left[\left(\frac{A}{2}\delta_{h,k} - B_{hk}\right)[(\mu_{i,i}(\boldsymbol{x}) + \mu_{i,i}(\boldsymbol{y}))\theta_{h,k}(\boldsymbol{x}) + (\theta_{i,i}(\boldsymbol{x}) + \theta_{i,i}(\boldsymbol{y}))\mu_{h,k}(\boldsymbol{x})] \right. \\ & \left. + B_{ik}[\theta_{i,h}(\boldsymbol{x})\mu_{h,k}(\boldsymbol{x}) + \mu_{i,h}(\boldsymbol{x})\theta_{h,k}(\boldsymbol{x}) + \theta_{i,h}(\boldsymbol{x})\mu_{i,h}(\boldsymbol{y})] - A\theta_{h,k}(\boldsymbol{x})\mu_{k,h}(\boldsymbol{x}) \right] \frac{1}{r} \Big\} \mathrm{d}S_x \, \mathrm{d}S_y \end{aligned} \tag{66}$$

6. Numerical implementation for planar cracks

The Galerkin BIE formulations (63), (64) and Eqs. (65), (66) constitute the basis of the implementation presented in this section.

6.1. Crack and COD representation

The (planar) surface Γ is interpolated using n_E triangular or quadrilateral boundary elements. The eth boundary element in physical space is mapped onto a parent element Δ_e using n_e shape functions N_k and interpolation nodes $\boldsymbol{y}^k$, according to

$$\boldsymbol{y} = \sum_{k=1}^{n_e} N_k(\xi_1, \xi_2)\boldsymbol{y}^k \quad (\xi_1, \xi_2) \in \Delta_e \tag{67}$$

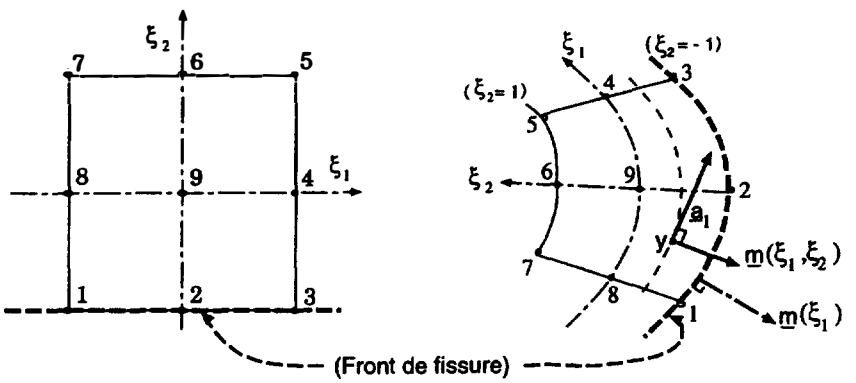

Fig. 2. Natural basis and local numbering of elements adjacent to the crack front; extension $\boldsymbol{\nu}(\xi_1, \xi_2)$ of the unit normal $\boldsymbol{\nu}(\xi_1)$ to $\partial\Gamma$.

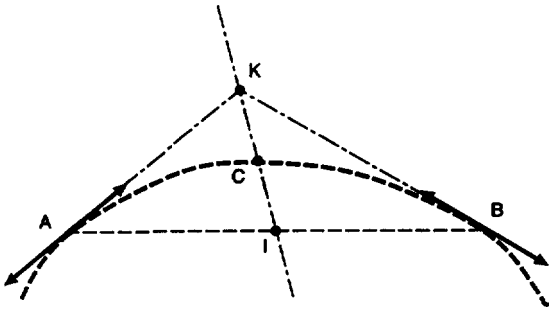

Fig. 3. Geometrical construction used to define a C^1 interpolation of the crack front: $AI = AB/2$ then $IC = IK/2$.

In this work, 6-noded triangles and 9-noded quadrangles are used (in particular, elements adjacent to the crack front are quarter-point 9-noded quadrangles). An isoparametric interpolation is used for the COD $\boldsymbol{\phi}$:

$$\boldsymbol{\phi}(\boldsymbol{y}) = \sum_{k=1}^{n_e} N_k(\xi_1, \xi_2)\boldsymbol{\phi}^{(k)} \quad \text{where} \quad \boldsymbol{y} = \boldsymbol{y}(\xi_1, \xi_2) \text{ through (67)} \tag{68}$$

6.2. Interpolation of the extension velocity

Let the global numbering of nodes be chosen such that $\boldsymbol{y}^1, \ldots, \boldsymbol{y}^{n_C}$ are the n_C interpolation nodes located on the crack front $\partial\Gamma$, and denote by $E(\partial\Gamma)$ the set of (9-noded, quadrilateral) boundary elements adjacent to $\partial\Gamma$. The local numbering of nodes for any such element is conventionally defined so that nodes 1, 2, 3 lie on the crack front, which is thus interpolated by the curvilinear segment ($\xi_2 = -1$) and using the usual one-dimensional quadratic shape functions (see Fig. 2).

$$S_1(\xi_1) = \xi_1(\xi_1 - 1)/2 \qquad S_2(\xi_1) = 1 - \xi_1^2 \qquad S_3(\xi_1) = \xi_1(\xi_1 + 1)/2 \tag{69}$$

Within this interpolation framework, a C^1 (i.e. with continuous unit tangent $\boldsymbol{\tau}$ and normal $\boldsymbol{\nu}$) interpolation of the crack front can be defined, as shown in Fig. 3 (the midside node C is constructed as indicated given the endpoints A, B and their tangents).

Now, a finite dimensional subspace Θ_{n_C} of the space Θ of admissible transformation velocities $\boldsymbol{\theta}$ is defined so as to satisfy two requirements:

(1) The trace on Γ of any $\boldsymbol{\theta} \in \Theta_{n_C}$ is zero outside $E(\partial\Gamma)$ (Fig. 4);

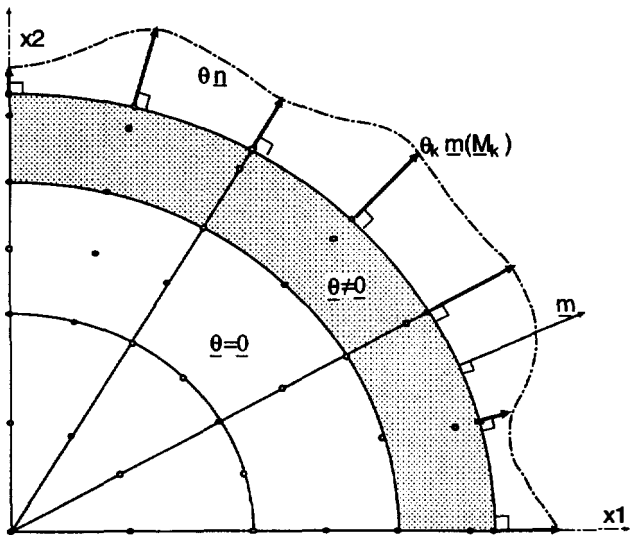

Fig. 4. Geometrical support and nodal values for the interpolation on Γ of extension velocities $\boldsymbol{\theta}$.

(2) Any $\boldsymbol{\theta} \in \Theta_{n_C}$ is a linear combination of the *normal* velocities $\theta_k = \theta_\nu(\boldsymbol{y}^k)$ at the crack front nodes:

$$\boldsymbol{\theta}(\boldsymbol{y}) = \sum_{k=1}^{n_C} \boldsymbol{B}^k(\boldsymbol{y})\theta_k \tag{70}$$

In order to do so, vector interpolation functions $\boldsymbol{B}^k$ $(1 \leqslant k \leqslant n_C)$ are defined as follows, in terms of the one-dimensional shape functions S_k given by (69)

$$\boldsymbol{B}^j(\boldsymbol{\xi}) = \frac{1}{2}(1-\xi_2)S_k(\xi_1)\left(\frac{-\boldsymbol{a}_1}{|\boldsymbol{a}_1|} \wedge \boldsymbol{e}_3\right) \tag{71}$$

where the *natural basis* $\boldsymbol{a}_\alpha(\xi_1, \xi_2)$ $(\alpha = 1, 2)$ on a given boundary element is defined by (Fig. 2)

$$\boldsymbol{a}_\alpha(\xi_1, \xi_2) = \frac{\partial}{\partial \xi_\alpha}\boldsymbol{y}(\xi_1, \xi_2) = \sum_{k=1}^{n_e} \frac{\partial N_k}{\partial \xi_\alpha}\boldsymbol{y}^k \quad (\alpha = 1, 2) \tag{72}$$

It is readily seen that the $\boldsymbol{B}^k$ have the following properties:

$$\boldsymbol{B}^k|_{\xi_2=1} = 0 \qquad \boldsymbol{B}^k(\boldsymbol{y}^\ell) = \delta_{k\ell}\boldsymbol{\nu}(\boldsymbol{y}^k) \qquad \boldsymbol{B}^k.\boldsymbol{e}_3 = 0 \tag{73}$$

The function $\boldsymbol{B}^2$ is depicted in Fig. 5.

6.3. Comments

Other definitions of the generating family $\{\boldsymbol{B}^k(\boldsymbol{y}),\ 1 \leqslant k \leqslant n_C\}$ of the finite-dimensional subspace Θ_{n_C} of Θ satisfying (73) could be proposed. The present one is relatively easy to implement, thanks to the fact that its geometrical support is reduced to the ring of boundary elements adjacent to the crack front.

Definition (71) implies that the (tangential) gradients of $\boldsymbol{\phi}$, $\tilde{\boldsymbol{\phi}}$ in the vicinity of the crack front are involved in the computation of the various integrals containing extension velocities.

It is also important to note that the trace on the crack front of any velocity $\boldsymbol{\theta} \in \Theta_{n_C}$ has the form:

$$\boldsymbol{\theta} = \theta_\nu(\xi_1)\boldsymbol{\nu}(\xi_1) \quad \text{with} \quad \theta_\nu(\xi_1) = \sum_{k=1}^{n_C} S_k(\xi_1)\theta_k \tag{74}$$

and is continuous over $\partial\Gamma$ thanks to the C^1 interpolation of $\partial\Gamma$ introduced.

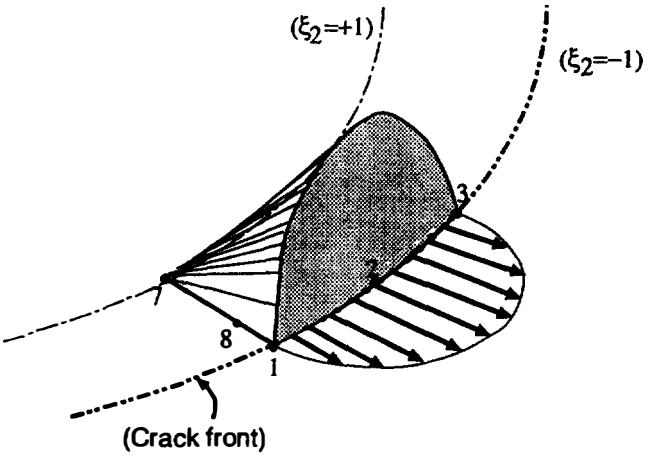

Fig. 5. Sketch of the vector interpolation function $\boldsymbol{B}^2$.

6.4. Discretized equations

The foregoing discretization approach results in the following steps for the discretized instantaneous crack extension problem.

6.4.1. Computation of the COD

The governing Galerkin formulations (63), (64) for the mode I and modes II–III crack equilibrium problems take the form:

$$\boldsymbol{B}_{33}\boldsymbol{\phi}_3 = \boldsymbol{L}_3 \begin{bmatrix} \boldsymbol{B}_{11} & \boldsymbol{B}_{12} \\ \boldsymbol{B}_{12} & \boldsymbol{B}_{22} \end{bmatrix} \begin{Bmatrix} \boldsymbol{\phi}_1 \\ \boldsymbol{\phi}_2 \end{Bmatrix} = \begin{Bmatrix} \boldsymbol{L}_1 \\ \boldsymbol{L}_2 \end{Bmatrix} \tag{75}$$

where

$$\boldsymbol{B}_{ij} = [\mathscr{B}(N_a\boldsymbol{e}_i, N_b\boldsymbol{e}_j)]_{1\leqslant a,b\leqslant n_N - n_C} \qquad \boldsymbol{L}_i = \{\langle N_a, \bar{t}_i\rangle_\Gamma\}_{1\leqslant a\leqslant n_N-n_C}^{\mathrm{T}}$$

$$\boldsymbol{\phi}_i = \{\phi_i^{(1)}, \ldots, \phi_i^{(n_N-n_C)}\}^{\mathrm{T}} = \{\phi_i(\boldsymbol{y}^{n_C+1}), \ldots, \phi_i(\boldsymbol{y}^{n_N})\}^{\mathrm{T}}$$

where n_N denotes the total number of nodes (note that according to the present global numbering convention of nodes, $\boldsymbol{\phi}(\boldsymbol{y}^1) = \cdots = \boldsymbol{\phi}(\boldsymbol{y}^{n_C}) = \boldsymbol{0}$).

6.4.2. COD derivative in a given crack extension

The governing Galerkin BIE formulation (38) for the nodal values $\overset{*}{\boldsymbol{\phi}}{}^{(b)}$ of the Lagrangian derivative of $\boldsymbol{\phi}$ in the extension velocity $\boldsymbol{B}^b$ is

$$[\boldsymbol{B}_{33}]\{\overset{*}{\boldsymbol{\phi}}{}_3^{(b)}\} = \{\overset{*}{\boldsymbol{L}}{}_3^{(b)}\} \begin{bmatrix} \boldsymbol{B}_{11} & \boldsymbol{B}_{12} \\ \boldsymbol{B}_{12} & \boldsymbol{B}_{22} \end{bmatrix} \begin{Bmatrix} \overset{*}{\boldsymbol{\phi}}{}_1^{(b)} \\ \overset{*}{\boldsymbol{\phi}}{}_2^{(b)} \end{Bmatrix} = \begin{Bmatrix} \overset{*}{\boldsymbol{L}}{}_1^{(b)} \\ \overset{*}{\boldsymbol{L}}{}_2^{(b)} \end{Bmatrix} \tag{76}$$

with the notations

$$\overset{*}{\boldsymbol{L}}{}_1^{(b)} = -[\mathscr{B}_{11}^{1(b)}]\{\boldsymbol{\phi}_1\} - [\mathscr{B}_{12}^{1(b)}]\{\boldsymbol{\phi}_2\} - \left\{\int_\Gamma (\nabla N_a \cdot \boldsymbol{B}^b)\bar{t}_1 \, \mathrm{d}S\right\}_{1\leqslant a\leqslant n_N-n_C,\, 1\leqslant b\leqslant n_C}$$

$$\overset{*}{\boldsymbol{L}}{}_2^{(b)} = -[\mathscr{B}_{21}^{1(b)}]\{\boldsymbol{\phi}_1\} - [\mathscr{B}_{22}^{1(b)}]\{\boldsymbol{\phi}_2\} - \left\{\int_\Gamma (\nabla N_a \cdot \boldsymbol{B}^b)\bar{t}_2 \, \mathrm{d}S\right\}_{1\leqslant a\leqslant n_N-n_C,\, 1\leqslant b\leqslant n_C}$$

$$\overset{*}{\boldsymbol{L}}{}_3^{(b)} = -[\mathscr{B}_{33}^{1(b)}]\{\boldsymbol{\phi}_3\} - \left\{\int_\Gamma (\nabla N_a \cdot \boldsymbol{B}^b)\bar{t}_3 \, \mathrm{d}S\right\}_{1\leqslant a\leqslant n_N-n_C,\, 1\leqslant b\leqslant n_C}$$

$$[\mathscr{B}_{ij}^{1(b)}] = [\mathscr{B}^1(N_a\boldsymbol{e}_i, N_c\boldsymbol{e}_j; \boldsymbol{B}^b)]_{1\leqslant a,c\leqslant n_N-n_C}$$

6.5. Energy release rate

Eq. (17) in discretized form, which governs the nodal unknown energy release rate values $\{G\} = \{G_1, \ldots, G_{n_C}\}^{\mathrm{T}}$, reads:

$$[K]\{G\} = \{\ell\} \tag{77}$$

having set

$$K_{ab} = \int_{\partial\Gamma} S_a S_b \, \mathrm{d}s \quad (1 \leqslant a, b \leqslant n_C)$$

$$\ell_b = -\frac{1}{2}\{\boldsymbol{\phi}_1, \boldsymbol{\phi}_2\} \begin{bmatrix} \mathscr{B}_{11}^{1(b)} & \mathscr{B}_{12}^{1(b)} \\ \mathscr{B}_{12}^{1(b)} & \mathscr{B}_{22}^{1(b)} \end{bmatrix} \begin{Bmatrix} \boldsymbol{\phi}_1 \\ \boldsymbol{\phi}_2 \end{Bmatrix} - \frac{1}{2}\{\boldsymbol{\phi}_3\}^{\mathrm{T}}[\mathscr{B}_{33}^{1(b)}]\{\boldsymbol{\phi}_3\} - \langle \nabla\boldsymbol{\phi} \cdot \boldsymbol{B}^b, \bar{\boldsymbol{t}}\rangle_\Gamma$$

6.6. Discretized rate problem

The symmetric $n_C \times n_C$ matrix $[Q]$ associated to the quadratic form $Q(\boldsymbol{\theta}, \boldsymbol{\theta})$ defined by (20) is computed using

$$\begin{aligned} Q_{ab} &= Q(\boldsymbol{B}^a, \boldsymbol{B}^b) \\ &= -\mathcal{B}(\overset{*}{\boldsymbol{\phi}}{}^{(a)}, \overset{*}{\boldsymbol{\phi}}{}^{(b)}) + \frac{1}{2}\mathcal{B}^2(\boldsymbol{\phi}, \boldsymbol{\phi}; \boldsymbol{B}^a, \boldsymbol{B}^b) - \int_{\partial\Gamma} G_c S_a S_b \kappa \, \mathrm{d}s \\ &\quad - \int_\Gamma \{(\nabla\boldsymbol{\phi}.\boldsymbol{B}^a).(\bar{\boldsymbol{t}}\,\mathrm{div}_S\,\boldsymbol{B}^b + \nabla\bar{\boldsymbol{t}}.\boldsymbol{B}^b) - (\nabla\boldsymbol{\phi}.\nabla\boldsymbol{B}^b.\boldsymbol{B}^a)\bar{\boldsymbol{t}}\}\,\mathrm{d}S \end{aligned} \tag{78}$$

The matrix $[Q]$ is then used to implement the stability (existence of actual extension velocity $\boldsymbol{\mu}$) and non-bifurcation (uniqueness of solution $\boldsymbol{\mu}$) criteria:

(1) A Choleski factorization is first performed on $[Q]$. If this operation terminates successfully, $[Q]$ is positive definite, which in turn means that the uniqueness criterion (26) is satisfied.

(2) If the Cholesky factorization is unsuccessful, the uniqueness criterion (26) is violated and the weaker, existence criterion (25) must be tested. In practical terms, one is led to test the positiveness of $\Sigma_{a,b} Q_{ab}\theta_a\theta_b$ for any $\{\boldsymbol{\theta}\} \geqslant \mathbf{0}$, which is in turn equivalent to testing the positiveness of $J(\boldsymbol{x}) = \Sigma_{a,b} Q_{ab} x_a^2 x_b^2$ without constraints on $\{\boldsymbol{x}\}$. In practice, one can apply an algorithm for unconstrained minimization to $J(\boldsymbol{x})$ (e.g. the conjugate gradient method). $J(\boldsymbol{x})$ either has a minimum equal to zero or has no lower bound. In the latter case, negative values of $J(\boldsymbol{x})$ should be encountered by the minimization algorithm. At the first such occurrence, the existence criterion is known to be violated.

6.7. Compute the actual extension velocity

If $[Q]$ is positive definite, the actual extension velocity $\boldsymbol{\mu} = \{\mu_1, \ldots, \mu_{n_C}\}^{\mathrm{T}}$ induced by a load rate $\bar{\boldsymbol{t}}'$ solves the linear system of equations:

$$[Q]\{\mu\} = \{f\} \qquad f_a = \int_\Gamma (\overset{*}{\boldsymbol{\phi}}{}^{(a)} - \nabla\boldsymbol{\phi}.\boldsymbol{B}^a).\bar{\boldsymbol{t}}'\,\mathrm{d}S \tag{79}$$

6.8. Computation of element integrals

The discretization process for the bilinear forms $\mathcal{B}(\boldsymbol{\phi}, \tilde{\boldsymbol{\phi}})$, $\mathcal{B}^1(\boldsymbol{\phi}, \tilde{\boldsymbol{\phi}}; \boldsymbol{\theta})$ and $\mathcal{B}^2(\boldsymbol{\phi}, \tilde{\boldsymbol{\phi}}; \boldsymbol{\theta}, \boldsymbol{\mu})$ involves integrations over Cartesian products of elements $E \times E'$. The typical form of such integrals is

$$I(E, E') = \int_E \int_{E'} \nabla\tilde{\boldsymbol{\phi}}(\boldsymbol{x}) : \boldsymbol{k}(\boldsymbol{x}, \boldsymbol{y}) : \nabla\boldsymbol{\phi}(\boldsymbol{y})\,\mathrm{d}S_y\,\mathrm{d}S_x \tag{80}$$

with

$$\begin{aligned} \boldsymbol{k}(\boldsymbol{x}, \boldsymbol{y}) &= \frac{1}{r}\boldsymbol{f} + \nabla\frac{1}{r}\cdot\{[\boldsymbol{\theta}(\boldsymbol{y}) - \boldsymbol{\theta}(\boldsymbol{x})]\boldsymbol{g}_1 + [\boldsymbol{\mu}(\boldsymbol{y}) - \boldsymbol{\mu}(\boldsymbol{x})]\boldsymbol{g}_2\} \\ &\quad + [\boldsymbol{\theta}(\boldsymbol{y}) - \boldsymbol{\theta}(\boldsymbol{x})].\nabla\nabla\frac{1}{r}.[\boldsymbol{\mu}(\boldsymbol{y}) - \boldsymbol{\mu}(\boldsymbol{x})]\boldsymbol{h} \end{aligned} \tag{81}$$

and $r = |\boldsymbol{y} - \boldsymbol{x}|$; $\boldsymbol{f}, \boldsymbol{g}_1, \boldsymbol{g}_2, \boldsymbol{h}$ are non-singular fourth-order tensor functions of $\boldsymbol{x}, \boldsymbol{y}$ which include when appropriate the presence of $\boldsymbol{\theta}, \boldsymbol{\mu}$.

In principle, three different types of situations arise: singular integration ($E = E'$), adjacent integration (E, E' are distinct but share a common edge or vertex) and regular integration (E, E' are completely disjoint). Adjacent integrations are specific to Galerkin boundary element methods and do not arise in collocation-type implementations. The integrand exhibits in the four-dimensional Cartesian product $E \times E'$ a singularity (which is weaker than the r^{-1} singularity arising in the singular integration case). This, in principle, mandates a proper, specific, numerical integration algorithm. In contrast to the ordinary singular and regular cases, adjacent integration algorithms are complex and not yet fully developed for 3D situations. This, and the fact that an improper integration scheme is expected to have lower adverse effects than in the singular ($E = E'$) case, led us to treat adjacent integrations in the same way as regular integrations, at least for the time being.

6.8.1. Case $E = E'$: singular integration

In this case, the various kernels $k(\boldsymbol{x}, \boldsymbol{y})$ are integrable over a *single* element (their order of singularity being r^{-1}). Hence, the double integral is treated as an inner singular integral over $\boldsymbol{y} \in E$ followed by an outer nonsingular integral over $\boldsymbol{x} \in E$. The outer integral is thus computed using Gauss points, which in turn implies that the inner integrals must be computed with the singular points $\boldsymbol{x}$ taken as the Gauss points used for the outer integral.

The evaluation of inner, singular, integrals for a fixed position of $\boldsymbol{x} \in E$ uses polar coordinates (ρ, φ) in the parent element Δ, centered at the antecedent $\boldsymbol{\eta} \in \Delta$ of $\boldsymbol{x}$ (Fig. 6), so that the antecedent $\boldsymbol{\xi}$ of $\boldsymbol{y}$ is given by

$$(\xi_1, \xi_2) = (\eta_1 + \rho \cos \varphi, \eta_2 + \rho \sin \varphi) \tag{82}$$

Then, auxiliary shape functions $\tilde{N}_m(\rho, \varphi; \boldsymbol{\eta})$ [2] are defined according to

$$N_m(\boldsymbol{\xi}) - N_m(\boldsymbol{\eta}) = \rho \tilde{N}_m(\rho, \varphi; \boldsymbol{\eta}) \tag{83}$$

(see Appendix A.4 for the 9-noded quadrilateral element). The following formulas can then be readily established:

$$\boldsymbol{y} - \boldsymbol{x} = \rho \hat{\boldsymbol{r}} = \rho \sum_{m=1}^{N_e} \tilde{N}_m(\rho, \varphi, \boldsymbol{\eta}) \qquad r = \rho \hat{r} = \rho |\hat{\boldsymbol{r}}|$$

$$\frac{1}{r} = \frac{1}{\rho} \frac{1}{\hat{r}} \qquad \boldsymbol{\nabla} \frac{1}{r} = -\frac{1}{\rho^2} \frac{\hat{\boldsymbol{r}}}{\hat{r}^3} \qquad \boldsymbol{\nabla}\boldsymbol{\nabla} \frac{1}{r} = \frac{1}{\rho^3} \left(\frac{-3\hat{\boldsymbol{r}} \otimes \hat{\boldsymbol{r}}}{\hat{r}^5} - \frac{\boldsymbol{I}}{\hat{r}^3} \right)$$

In a similar fashion, auxiliary vector interpolation functions $\hat{\boldsymbol{B}}^m$ are defined according to

$$\boldsymbol{B}^m(\boldsymbol{\xi}) - \boldsymbol{B}^m(\boldsymbol{\eta}) = \rho \hat{\boldsymbol{B}}^m(\rho, \varphi; \boldsymbol{\eta}) \tag{84}$$

(the expression for $\hat{B}_j^m$ is established in Appendix A.4). Eq. (81) can thus be recast as combinations of

$$\boldsymbol{k}(\boldsymbol{y} - \boldsymbol{x}) = \frac{1}{\rho} \left\{ \frac{1}{\hat{r}} \boldsymbol{f} - \frac{\hat{\boldsymbol{r}}}{\hat{r}^3} \cdot (\hat{\boldsymbol{B}}^m \boldsymbol{g}_1 + \hat{\boldsymbol{B}}^n \boldsymbol{g}_2) + \hat{\boldsymbol{B}}^m \cdot \left(\frac{-3\hat{\boldsymbol{r}} \otimes \hat{\boldsymbol{r}}}{\hat{r}^5} - \frac{\boldsymbol{I}}{\hat{r}^3} \right) \cdot \hat{\boldsymbol{B}}^n \boldsymbol{h} \right\}$$

Finally, the differential area element $\mathrm{d}S_y$ is given by

$$\mathrm{d}S_y = J(\boldsymbol{\xi})\, \mathrm{d}\boldsymbol{\xi} = J(\boldsymbol{\xi}) \rho\, \mathrm{d}\rho\, \mathrm{d}\varphi$$

($J(\boldsymbol{\xi})$: jacobian of the mapping $\boldsymbol{\xi} \to \boldsymbol{y}(\boldsymbol{\xi})$). The quantity $\boldsymbol{k}(\boldsymbol{y} - \boldsymbol{x})\, \mathrm{d}S_y$ is then nonsingular in the (ρ, φ) coordinates, and can be integrated numerically, using a subdivision of the parent element Δ_e into three (triangular elements) or four (quadrangular elements).

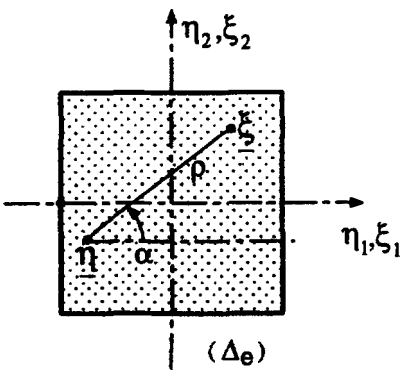

Fig. 6. Singular integration: polar coordinates centered at $\boldsymbol{\eta}$ and element subdivision into triangles.

6.9. Regular integration

The regular double element integrals (E, E' disjoint) and the simple surface element integrals are evaluated using ordinary Gaussian quadrature techniques.

6.10. Crack front singularity of $\nabla\phi$

It is taken into account using quadrilateral quarter-node elements along the crack front, allowing to use Gaussian quadrature in that case also.

7. Numerical examples

In this section, the concepts introduced in the foregoing development are illustrated and tested on three numerical examples where comparisons with exact solutions are possible. The configurations considered are: (i) elliptical crack under uniform tension; (ii) circular crack under torsional load; and (iii) circular crack with equal and opposite concentrated forces on the normal axis. In each case, the crack is embedded in an infinite elastic body.

The boundary element meshes are made of n_c concentric rings, each containing n_f elements; the notation $\mathcal{M}(n_f, n_c)$ is used for such meshes (for example, Fig. 7 displays the first quadrant of $\mathcal{M}(12, 3)$).

All numerical results presented below were obtained for the value $\nu = 0.3$ of the Poisson ratio. They often appear as 'root mean square (RMS)' errors on some distributed quantity x:

$$e^2_{\mathrm{RMS}} = \frac{\sum_{i=1}^{N} (x_i^{\mathrm{computed}} - x_i^{\mathrm{exact}})^2}{\sum_{i=1}^{N} (x_i^{\mathrm{exact}})^2}$$

where x_i are the nodal values associated with x and N is equal to either $n_N - n_C$ (e.g. for $x = \phi$) or n_C (e.g. for $x = G$).

7.1. Elliptical crack under uniform loading

The problem of an elliptical plane crack Γ (center O, axes $a \geq b$) embedded in an infinite elastic body and subjected to an arbitrary uniform loading has an exact solution (see e.g. [26]). For the particular case of uniform tension ($\underline{t} = p\boldsymbol{e}_3$, mode I problem), one has

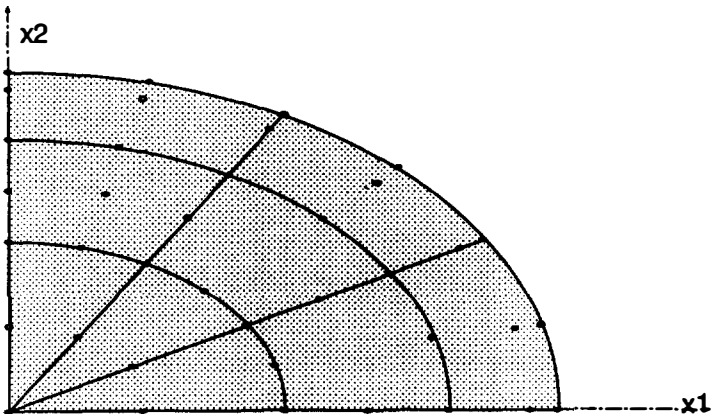

Fig. 7. Boundary element mesh $\mathcal{M}(12, 3)$ for an elliptical crack (first quadrant).

$$\phi_3 = \frac{(1-\nu)p}{\mu}\frac{b}{E(k)}\left(1-\frac{x_1^2}{a^2}-\frac{x_2^2}{b^2}\right)^{1/2}$$

$$G = p^2\frac{1-\nu^2}{E}\frac{\pi b}{E^2(k)}(1-k^2\cos^2\alpha)^{1/2}$$

where $E(k)$ denotes the complete elliptic integral of first kind:

$$E(k) = \int_0^{\pi/2}(1-k^2\cos^2\alpha)^{1/2}\,\mathrm{d}\alpha \qquad k^2 = 1-\frac{b^2}{a^2}$$

The particular case $a = b$ gives the well-known solution for a circular crack:

$$\phi_3 = \frac{2p(1-\nu)}{\mu\pi}(a^2-x_1^2-x_2^2)^{1/2} \qquad G = \frac{1-\nu^2}{E}\frac{4}{\pi}p^2a$$

from which it follows that

$$W(b,\,p) = \frac{8}{3}\frac{1-\nu^2}{E}p^2b^3 \qquad \frac{\mathrm{d}^2}{\mathrm{d}b^2}W(b,\,p) = 16\frac{1-\nu^2}{E}p^2b \tag{85}$$

A similar, more lengthy, solution is available for combined uniform tension and shear (mixed-mode problem).

Fig. 8 displays RMS errors on ϕ_3 for several meshes (circular crack, mode I loading) while the RMS errors on COD and potential energy at equilibrium are shown in Fig. 9 (mesh $\mathcal{M}(12, 3)$, aspect ration a/b ranging between 1 and 8.5, mode I loading). Although the latter mesh is not very fine, the RMS errors (which increase with a/b) are acceptable even for the larger aspect ratios, i.e. the most distorted meshes. Computed and exact distributions of G along the crack front are plotted in Fig. 10 for various values of a/b.

Fig. 11 displays the RMS errors on G obtained using either the present θ-integral approach or COD extrapolation (i.e. evaluated from the stress intensity factors K_{I}, K_{II}, K_{III} by means of Irwin's formula), with the same geometrical data as before, for a mixed-mode loading configuration. One notices that the RMS error obtained using the present θ-integral approach varies between about 0.5% and 2% (for the largest aspect ratio $a/b = 8.5$) and that the RMS error on G using extrapolation is about three times higher for any value of a/b.

The computed and exact values of the second-order derivative $\mathrm{d}^2W/\mathrm{d}b^2$ of the potential energy, for the case of a circular crack ($a = b$), are presented in Fig. 12. The computed value is obtained by applying the matrix $[Q]$ (78) of the rate problem for a unit circular extension $\theta_\nu(s) = 1$:

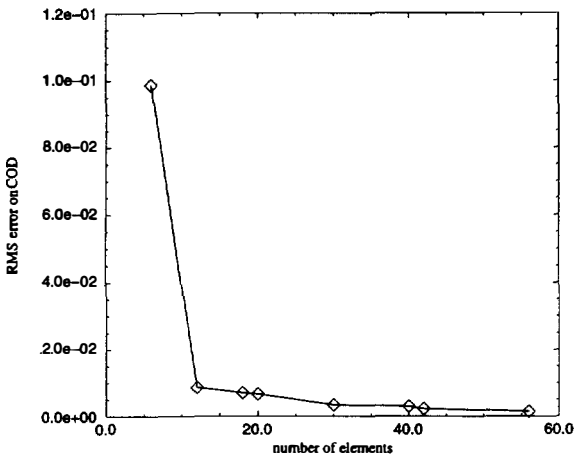

Fig. 8. Example 1: RMS error on ϕ_3 for several meshes.

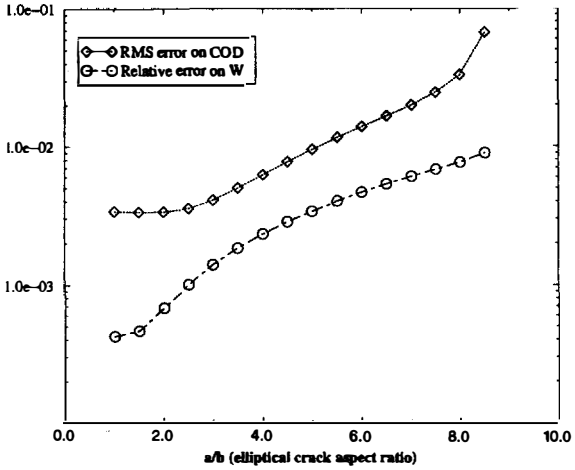

Fig. 9. Example 1: RMS errors on ϕ_3 and $W(\Gamma, \bar{t})$ for mesh $\mathcal{M}(12, 3)$ and various values of crack aspect ratio a/b.

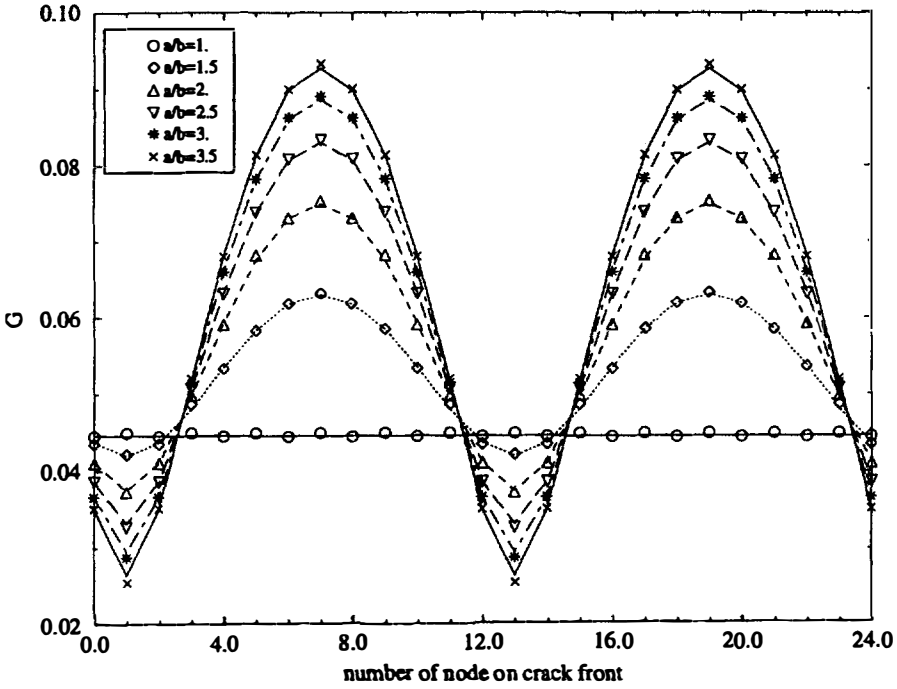

Fig. 10. Example 1: computed and exact distributions of G along the crack front for several aspect ratio values (mode I loading).

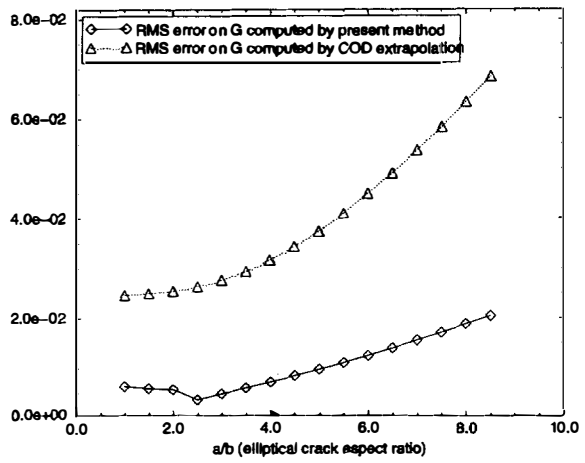

Fig. 11. Example 1: RMS error on $G(s)$ for mesh $\mathcal{M}(12, 3)$ and various values of a/b (mixed-mode loading).

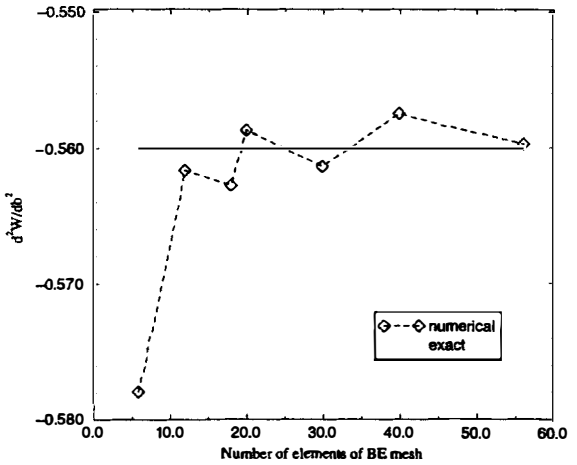

Fig. 12. Example 1: computed and exact values of d^2W/da^2, for several meshes.

$$(W_{,bb})_{\text{calculate}} = \sum_{i,j} Q_{ij} \tag{86}$$

whereas the exact value is given by (85). A good agreement between the two values is observed (relative error less than 1% except for the coarsest mesh).

7.2. Circular crack under torsional loading

This is a mode III situation: a circular crack Γ (radius: a) is loaded by $\bar{t}_1 = px_2/a$, $\bar{t}_2 = -px_1$. The exact solution [26] is

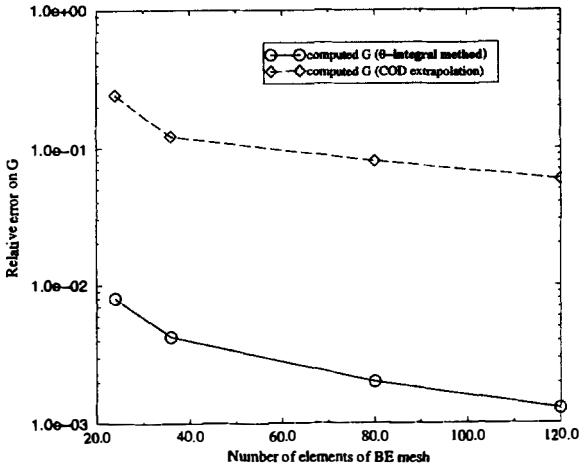

Fig. 13. Example 2: RMS error on $G(s)$ obtained by extrapolation of ϕ_1, ϕ_2 and by the present method.

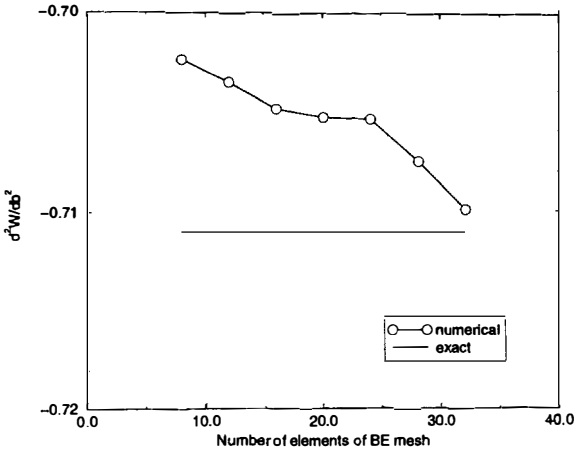

Fig. 14. Example 2: computed and exact values of $W_{,aa}$ for various meshes.

$$G = \frac{8}{9\pi\mu} p^2 a^3 \qquad W(a, p) = -\frac{16}{45\mu} p^2 a^5 \qquad W_{,aa} = -\frac{64}{9\mu} p^2 a^3 \tag{87}$$

Results for the RMS error on $G(s)$ obtained using either the present domain derivative-based approach or K_{III} evaluated by means of COD extrapolation of ϕ_1, ϕ_2 are shown in Fig. 13. The present approach is seen to provide more accurate values of G. Fig. 14 displays exact and computed values of $W_{,aa}$ (the latter again obtained from (86)). A good agreement is observed, the relative error being well below 1% except for the coarsest mesh.

7.3. Circular crack with equal and opposite concentrated forces on the normal axis

A circular crack (radius a) is loaded by two equal and opposite point forces $\pm P\boldsymbol{e}_3$ applied at points $(0, 0, \pm h)$ (Fig. 15). The exact solution for G to this axisymmetric, mode I problem is known [26]:

$$G = \frac{1-\nu^2}{E} \frac{P^2}{(\pi h)^3} \frac{\alpha(\kappa + \alpha^2)}{(1+\alpha^2)^4} \quad \text{with} \quad \alpha = \frac{a}{h}, \qquad \kappa = \frac{2-\nu}{1-\nu} \tag{88}$$

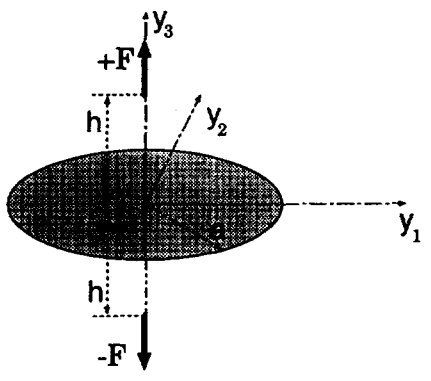

Fig. 15. Circular crack with equal and opposite concentrated loads.

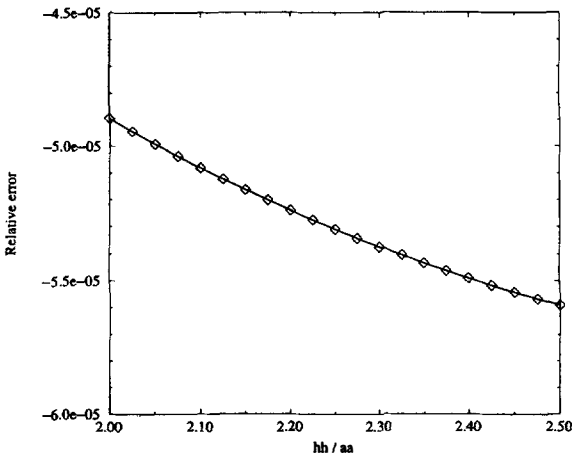

Fig. 16. Example 3: relative error on the potential energy at equilibrium.

One can easily show from (88) that the exact solution for G gives

$$\frac{dG}{d\alpha} = \frac{(1-\nu^2)P^2}{E(\pi h)^3} \frac{\alpha^2+\kappa}{(1+\alpha^2)^5} [-3\alpha^4 + (7\kappa - 5)\alpha^2 + \kappa]$$

and hence that

$$\frac{dG}{d\alpha} \begin{cases} <0 (\alpha > \alpha_m) \\ >0 (0 < \alpha < \alpha_m) \end{cases} \quad \text{with} \quad \alpha_m^2 = \frac{\sqrt{(7\kappa-5)^2 + 12\kappa} + 5 - 7\kappa}{6} \tag{89}$$

(with $\alpha_m = (a/h)_m \approx 0.43939$, or $\alpha_m^{-1} = (h/a)_m \approx 2.2759$ for $\nu = 0.3$). As a consequence, a circular crack front extension is stable for $a > h/\alpha_m$ but unstable for $a < h/\alpha_m$. In the stable case, uniqueness of the crack front extension velocity $\theta_v(s)$ is not guaranteed since the exact solution (88) does not address the possibility of non-circular extensions. Moreover, assuming that the load parameter P is such that $G = G_c$, the Griffith criterion leads to the following relation between the radius and load increments da and dP:

$$da = 2\frac{dP}{P} \frac{\alpha(1+\alpha^2)(\kappa+\alpha^2)}{3\alpha^4 + (7\kappa-5)\alpha^2 - \kappa} \tag{90}$$

which provides a means to compare the computed extension velocity $\mu_v(s)$ against an exact solution. This and the occurrence of either stable or unstable extension depending on the ratio a/h constitute the main interesting features of this example.

Fig. 16 displays the relative error for the potential energy at equilibrium $W(P, a)$,with $2 \leq h/a \leq 2.5$, using the mesh $\mathcal{M}(12, 3)$ (the exact solution for W is evaluated from (88) using

$$\frac{\partial W}{\partial a} = -2\pi a G(P, a)$$

The RMS error on G obtained in the same conditions, using either the present approach or K_I evaluated by means of kinematic extrapolation of ϕ_3 is shown in Fig. 17. Here again, the present approach provides superior accuracy.

The positive definiteness of the matrix $[Q]$ (uniqueness criterion (26) for stable crack extension, in discretized form) has been tested using the Choleski factorization. This test has been performed using the mesh $\mathcal{M}(12, 3)$, for $h/a = 2 + 0.005i$, $0 \leq i \leq 100$ (each value of h/a requiring to perform the entire solution process). Then, a refined scanning has been made for the interval $2.26 \leq h/a \leq 2.28$ in which the value of a/b for which loss of positive-definiteness for $[Q]$ was observed in the previous procedure lies: for each of the three meshes $\mathcal{M}(8, 2)$, $\mathcal{M}(12, 3)$ and $\mathcal{M}(16, 5)$, the matrix $[Q]$ has been set up for $h/a = 2.26 + 0.0005i$, $0 \leq i \leq 40$ (each value of h/a requiring again to perform the entire solution process). Table 1 displays the brackets found for the transition

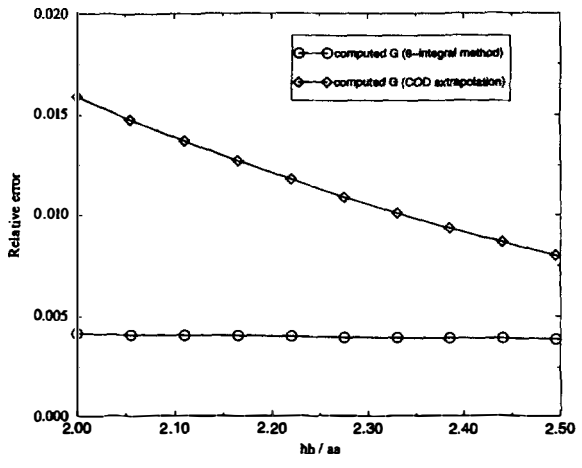

Fig. 17. Example 3: relative error on G using either the present approach or kinematic extrapolation of ϕ_3.

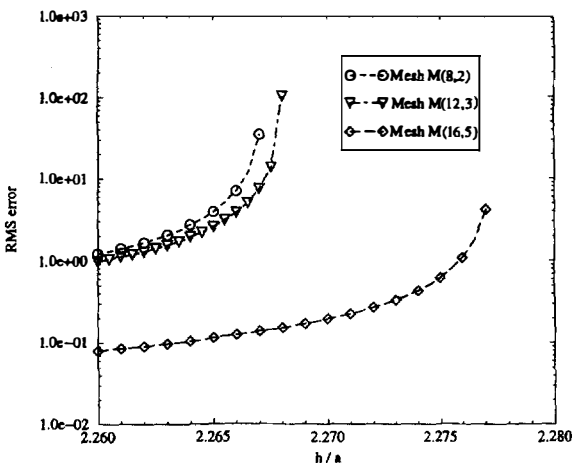

Fig. 18. Example 3: RMS error for the crack front extension velocity: meshes $\mathcal{M}(8, 2)$, $\mathcal{M}(12, 3)$, $\mathcal{M}(16, 5)$, 2, $26 \leq h/a \leq 2, 28$.

Table 1
Bracketing of the transition value $(h/a)_m$

Mesh	Brackeying	Relative error
$\mathcal{M}(8, 2)$	$2.267 \leq \alpha_m^{-1} \leq 2.2675$	$\leq 3.910^{-3}$
$\mathcal{M}(12, 3)$	$2.268 \leq \alpha_m^{-1} \leq 2.2685$	$\leq 3.510^{-3}$
$\mathcal{M}(16, 5)$	$2.277 \leq \alpha_m^{-1} \leq 2.275$	$\leq 7.010^{-4}$

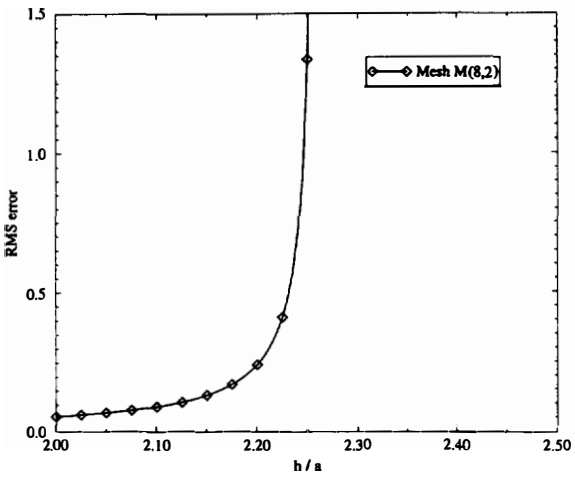

Fig. 19. Example 3: RMS error for the crack front extension velocity: mesh $\mathcal{M}(8, 2)$, $2 \leq h/a \leq 25$.

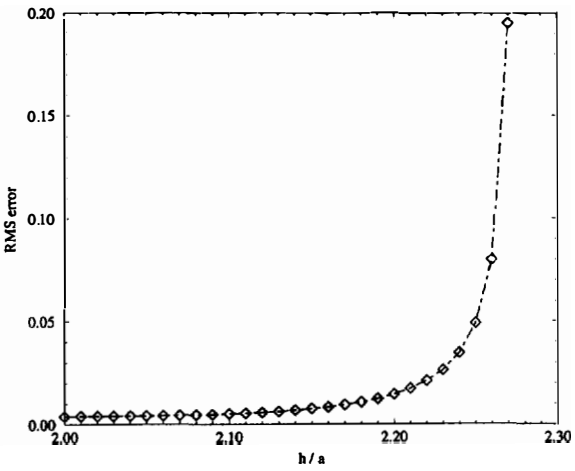

Fig. 20. Example 3: RMS error for the crack front extension velocity: mesh $\mathcal{M}(16, 5)$, $2 \leq h/a \leq 2.3$.

value $(h/a)_m$, which compares very well with the theoretical value even for the relatively coarse mesh $\mathcal{M}(8, 2)$. These results show indirectly that the present θ-integral method leads to a very good evaluation of the second-order energy derivatives.

Next, in the cases where $[Q]$ is found not to be positive definite, the existence criterion (25) is tested. For the present example, this test proved always negative, so that instantaneous crack extension is either stable and unique (hence circular), or unstable. This confirms that $(h/a)_m$ given by (89) corresponds to the transition between stable and unstable extensions in general (i.e. not only for circular extensions), and that the comparison with the value of $(h/a)_m$ estimated from the positive-definiteness of $[Q]$ is valid.

Fig. 18 displays, for the meshes $\mathcal{M}(8, 2)$, $\mathcal{M}(12, 3)$ and $\mathcal{M}(16, 5)$, the RMS error on the extension velocity $\boldsymbol{\mu}$ computed by solving the rate problem (24) when $[Q]$ is positive definite, for $2.26 \leq h/a \leq 2.28$ close to $(h/a)_m$ (the exact solution is provided by (90)). One observes the progressive degradation of the conditioning of $[Q]$ as h/a approaches $(h/a)_m$. Sufficiently away from $h/a = (h/a)_m$, the numerical solution to the instantaneous crack extension problem reproduces very well the circular extension given by the analytical solution (90). Figs. 19 and 20 display RMS errors on $\mu_\nu(s)$ (using the mesh $\mathcal{M}(8, 2)$ with $2 \leq h/a \leq 2.5$, and using the mesh $\mathcal{M}(16, 5)$ with $2 \leq h/a \leq 2.3$, respectively). Finally, the relative errors on (a) $W(a, P)$, (b) $G(s)$ computed using COD

Table 2
Example 3: relative errors on (a) $W(a, P)$, (b) $G(s)$ computed using COD extrapolation, (c) $G(s)$ computed using the present method, and (d) the extension velocity $\mu_\nu(s)$ for several meshes and $a/h = 0.5$

Mesh	$\Delta W/W$	$\frac{\|\Delta G_\theta\|_{L^2}}{\|G\|_{L^2}}$	$\frac{\|\Delta G_{\text{extrapol}}\|_{L^2}}{\|G\|_{L^2}}$	$\frac{\|\Delta \mu\|_{L^2}}{\|\mu\|_{L^2}}$
$\mathcal{M}(8,2)$	2.905E − 03	1.975E − 02	5.463E − 02	2.677E − 02
$\mathcal{M}(12, 2)$	−1.704E − 04	6.261E − 04	5.032E − 02	1.919E − 02
$\mathcal{M}(12, 3)$	3.823E − 05	7.897E − 03	2.910E − 02	1.965E − 02
$\mathcal{M}(16, 4)$	−3.721E − 04	3.996E − 03	2.173E − 02	4.262E − 03
$\mathcal{M}(16, 5)$	−7.176E − 04	3.789E − 03	2.142E − 02	4.466E − 03

extrapolation, (c) $G(s)$ computed using the present method, and (d) the extension velocity $\mu_v(s)$ are presented in Table 2 for several meshes and $a/h = 0.5$.

Appendix A

A.1. Surface gradient and divergence

Let $(\boldsymbol{a}_1, \boldsymbol{a}_2)$ denote the natural basis defined by (72) and define:

$$g_{\alpha\beta} = \boldsymbol{\alpha}_\alpha . \boldsymbol{a}_\beta \quad (\alpha, \beta = 1, 2) \qquad \hat{g} = g_{11} g_{22} - g_{12}^2 \tag{A.1}$$

The surface gradient of a scalar function $f(\boldsymbol{\xi})$ defined on a boundary element ($\boldsymbol{\xi} \in \Delta_e$) is given by

$$\boldsymbol{\nabla}_S f = f_{,\alpha} \boldsymbol{\alpha}^\alpha = f_{,\alpha} g^{\alpha\beta} \boldsymbol{a}_\beta = f_{,\alpha} g^{\alpha\beta} (\boldsymbol{a}_\beta . \boldsymbol{e}_r) \boldsymbol{e}_r \tag{A.2}$$

(where $g^{\alpha\beta}$ are the contravariant components associated with the covariant components defined by (A.1). One can introduce the Cartesian components $D_r f$ of $\boldsymbol{\nabla}_S f$:

$$D_r f = D_r \tilde{f} = \boldsymbol{\nabla}_S \tilde{f} . \boldsymbol{e}_r \tag{A.3}$$

Then, the surface divergence and surface gradient of a vector field $\boldsymbol{u}(\boldsymbol{\xi}) = u_r(\boldsymbol{\xi}) \boldsymbol{e}_r$ defined in terms of Cartesian components can be expressed, using the notation (A.3), as

$$D_r u_r = \boldsymbol{\nabla}_S \tilde{u}_r . \boldsymbol{e}_r = u_{r,\alpha} g^{\alpha\beta} (\boldsymbol{a}_\beta . \boldsymbol{e}_r)$$
$$D_p u_q = \boldsymbol{\nabla}_S \tilde{u}_q . \boldsymbol{e}_p = u_{q,\alpha} g^{\alpha\beta} (\boldsymbol{a}_\beta . \boldsymbol{e}_p)$$

A.2. Proof of symmetry of expression (39)

The proof uses some results from differential calculus on surfaces [11]. The following integration by parts formula holds:

$$\begin{aligned} &\int_\Gamma v^\alpha_{;\alpha} \, \mathrm{d}S = \int_{\partial\Gamma} v^\alpha \boldsymbol{\nu}_\alpha \, \mathrm{d}s \\ &\int_\Gamma f v^\alpha_{;\alpha} \, \mathrm{d}S = \int_{\partial\Gamma} f v^\alpha \boldsymbol{\nu}_\alpha \, \mathrm{d}s - \int_\Gamma f_{,\alpha} v^\alpha \, \mathrm{d}S \end{aligned} \tag{A.4}$$

where $\boldsymbol{v}_{;\beta}$ denotes the covariant derivative of a vector field $\boldsymbol{v}$:

$$\boldsymbol{v} = U^\alpha \boldsymbol{a}_\alpha \qquad \boldsymbol{v}_{;\beta} = [v^\alpha_{,\beta} + v^\gamma \Gamma^\alpha_{\gamma\beta}] \boldsymbol{a}_\alpha \otimes \boldsymbol{a}^{*\beta}$$

In addition, the following identity holds for any vector field tangent to Γ:

$$v^\beta_{;\alpha;\beta} - v^\beta_{;\beta;\alpha} = K \sqrt{\hat{g}} v_\alpha \tag{A.5}$$

(K: total curvature). For scalar fields f, partial and covariant derivatives coincide, so that

$$f_{;\alpha\beta} = f_{;\beta\alpha}$$

To settle the issue at hand, one has to investigate the symmetry in $(\boldsymbol{\theta}, \boldsymbol{\mu})$ of

$$\mathscr{E} = \int_\Gamma \{ (\boldsymbol{\nabla}\boldsymbol{\phi} . \boldsymbol{\theta}) . (\boldsymbol{\nabla}\bar{\boldsymbol{t}} . \boldsymbol{\mu} + \bar{\boldsymbol{t}} \, \mathrm{div}_S \, \boldsymbol{\mu}) - (\boldsymbol{\nabla}\boldsymbol{\phi} . \boldsymbol{\nabla}\boldsymbol{\mu} . \boldsymbol{\theta}) . \bar{\boldsymbol{t}} \} \, \mathrm{d}S \tag{A.6}$$

To this end, $\mathscr{E}$ is now reformulated by application of identities (A.4) and (A.5). On the one hand, one has

$$\int_\Gamma (\nabla\boldsymbol{\phi}\,.\,\boldsymbol{\theta})\bar{\boldsymbol{t}}\,\mathrm{div}_S\,\boldsymbol{\mu}\,\mathrm{d}S = \int_\Gamma \phi^i_{;\alpha}\theta^\alpha \bar{t}_i \mu^\beta_{;\beta}\,\mathrm{d}S$$

$$= -\int_\Gamma \phi^i(\theta^\alpha \bar{t}_i \mu^\beta_{;\beta})_{;\alpha}\,\mathrm{d}S$$

$$= -\int_\Gamma \phi^i(\theta^\alpha_{;\alpha}\bar{t}_i\mu^\beta_{;\beta} + \theta^\alpha \bar{t}_{i;\alpha}\mu^\beta_{;\beta} + \theta^\alpha \bar{t}_i \mu^\beta_{;\beta;\alpha})\,\mathrm{d}S$$

$$= -\int_\Gamma \phi^i(\theta^\alpha_{;\alpha}\bar{t}_i\mu^\beta_{;\beta} + \theta^\alpha \bar{t}_{i;\alpha}\mu^\beta_{;\beta} + \theta^\alpha \bar{t}_i u^\beta_{;\alpha;\beta} - \theta^\alpha \bar{t}_i \mu^\alpha Kg)\,\mathrm{d}S$$

$$= \int_\Gamma ((\phi^i\theta^\alpha \bar{t}_i)_{;\beta}\mu^\beta_{;\alpha} - \phi^i \bar{t}_i \theta^\alpha_{;\alpha}\mu^\beta_{;\beta} - \phi^i\theta^\alpha \bar{t}_{i;\alpha}\mu^\beta_{;\beta} + \phi^i \bar{t}_i \theta^\alpha \mu^\alpha Kg)\,\mathrm{d}S$$

$$= \int_\Gamma \{\phi^i_{;\beta}\theta^\alpha \bar{t}_i \mu^\beta_{;\alpha} + \phi^i \bar{t}_{i;\beta}[\theta^\alpha \mu^\beta_{;\alpha} - \theta^\beta \mu^\alpha_{;\alpha}] + \phi^i \bar{t}_i[\theta^\alpha \mu^\alpha Kg + \theta^\alpha_{;\beta}\mu^\beta_{;\alpha} - \theta^\alpha_{;\alpha}\mu^\beta_{;\beta}]\}\,\mathrm{d}S$$

Similarly, one has

$$\int_\Gamma (\nabla\boldsymbol{\phi}\,.\,\boldsymbol{\theta}).(\nabla\bar{\boldsymbol{t}}\,.\,\boldsymbol{\mu})\,\mathrm{d}S = \int_\Gamma \phi^i_{;\alpha}\theta^\alpha \bar{t}_{i;\beta}\mu^\beta\,\mathrm{d}S$$

$$= -\int_\Gamma \phi^i(\theta^\alpha \bar{t}_{i;\beta}\mu^\beta)_{;\alpha}\,\mathrm{d}S$$

$$= -\int_\Gamma \phi^i(\theta^\alpha_{;\alpha}\bar{t}_{i;\beta}\mu^\beta + \theta^\alpha \bar{t}_{i;\beta}\mu^\beta_{;\alpha} + \theta^\alpha \bar{t}_{i;\beta;\alpha}\mu^\beta)\,\mathrm{d}S$$

$$= -\int_\Gamma \phi^i(\theta^\alpha_{;\alpha}\bar{t}_{i;\beta}\mu^\beta + \theta^\alpha \bar{t}_{i;\beta}\mu^\beta_{;\alpha} + \theta^\alpha \bar{t}_{i;\alpha;\beta}\mu^\beta)\,\mathrm{d}S$$

$$= \int_\Gamma \{(\phi^i\theta^\alpha\mu^\beta)_{;\beta}\bar{t}_{i;\alpha} - \phi^i\theta^\alpha_{;\alpha}\bar{t}_{i;\beta}\mu^\beta - \phi^i\theta^\alpha \bar{t}_{i;\beta}\mu^\beta_{;\alpha}\}\,\mathrm{d}S$$

$$= \int_\Gamma \{\phi^i_{;\beta}\theta^\alpha\mu^\beta \bar{t}_{i;\alpha} + \phi^i \bar{t}_{i;\beta}[\theta^{\beta;\alpha}\mu^\alpha + \theta^\beta\mu^\alpha_{;\alpha} - \theta^\alpha_{;\alpha}\mu^\beta - \theta^\alpha\mu^\beta_{;\alpha}\}\,\mathrm{d}S$$

Note that in the above formula $\bar{t}_i$ is a *Cartesian* component of $\bar{\boldsymbol{t}}$ and can thus be treated as a scalar, hence $\bar{t}_{i;\alpha\beta} = \bar{t}_{i;\beta\gamma}$.

Substitution of the last two equations into (A.6) then results in (61).

A.3. Expression of $\mathscr{B}(\boldsymbol{\phi}, \tilde{\boldsymbol{\phi}})$ for a planar crack

An explicit expression of $\mathscr{B}(\boldsymbol{\phi}, \tilde{\boldsymbol{\phi}})$, defined by (53), is sought for the special case of a planar crack: the surface Γ lies in the plane $(O\boldsymbol{e}_1\boldsymbol{e}_2)$, and $\boldsymbol{n} = \boldsymbol{e}_3$. The bilinear form $\mathscr{B}(\boldsymbol{\phi}, \tilde{\boldsymbol{\phi}})$ is thus given by

$$\mathscr{B}(\boldsymbol{\phi}, \tilde{\boldsymbol{\phi}}) = \int_\Gamma \int_\Gamma B_{ikqs}(\boldsymbol{x}, \boldsymbol{y}) e_{fq} \tilde{\phi}_{i,f}(\boldsymbol{x}) e_{hs} \phi_{k,h}(\boldsymbol{y})\,\mathrm{d}S_x\,\mathrm{d}S_y$$

where $e_{ab} \equiv e_{3ab}$ is the two-dimensional permutation symbol, i.e. $e_{11} = e_{22} = 0$, $e_{12} = -e_{21} = 1$ (the indices f, q, h, s here range in $\{1, 2\}$ only). Then, using Eq. (47) together with the fact that $r_{,3} = 0$ for $\boldsymbol{x}, \boldsymbol{y} \in \Gamma$ (the crack is planar) and the identity

$$e_{ab}e_{cd} = \delta_{ac}\delta_{bd} - \delta_{ad}\delta_{bc}$$

one obtains

$$\mathcal{B}(\boldsymbol{\phi}, \tilde{\boldsymbol{\phi}}) = \frac{\mu}{4\pi(1-\nu)} \int_\Gamma \int_\Gamma \left\{ \tilde{\phi}_{3,h}(\boldsymbol{x})\phi_{3,h}(\boldsymbol{y}) - \frac{1+\nu}{2}\, \tilde{\phi}_{3,f}(\boldsymbol{x})\phi_{3,h}(\boldsymbol{y}) r_{,f} r_{,h} \right\} \frac{1}{r}\, dS_x\, dS_y$$
$$+ \frac{\mu}{8\pi} \int_\Gamma \int_\Gamma \left[\tilde{\phi}_{i,h}(\boldsymbol{x})\phi_{k,h}(\boldsymbol{y}) \frac{\delta_{ik} + r_{,i} r_{,k}}{r} + \tilde{\phi}_{i,k}(\boldsymbol{x})\phi_{k,i}(\boldsymbol{y}) \frac{1}{r} \right] dS_x\, dS_y$$
$$+ \frac{\mu\nu}{4\pi(1-\nu)} \int_\Gamma \int_\Gamma \tilde{\phi}_{i,i}(\boldsymbol{x})\phi_{k,k}(\boldsymbol{y}) \frac{1}{r}\, dS_x\, dS_y \tag{A.7}$$

This expression can be recast in a simpler form, using the following relations:

$$\int_\Gamma \int_\Gamma \tilde{\phi}_{i,k}(\boldsymbol{x})\phi_{k,i}(\boldsymbol{y}) \frac{1}{r}\, dS_x\, dS_y = -\int_\Gamma \int_\Gamma (\tilde{\phi}_i(\boldsymbol{x}) - \tilde{\phi}_i(\boldsymbol{y}))(\phi_k(\boldsymbol{y}) - \phi_i(\boldsymbol{x})) \left(\frac{1}{r}\right)_{,ik} dS_x\, dS_y$$
$$= \int_\Gamma \int_\Gamma \tilde{\phi}_{i,i}(\boldsymbol{x})\phi_{k,k}(\boldsymbol{y}) \frac{1}{r}\, dS_x\, dS_y \tag{A.8}$$

$$\int_\Gamma \int_\Gamma \tilde{\phi}_{i,h}(\boldsymbol{x})\phi_{k,h}(\boldsymbol{y}) \frac{r_{,i} r_{,k}}{r}\, dS_x\, dS_y = \int_\Gamma \int_\Gamma \tilde{\phi}_{i,h}(\boldsymbol{x})\phi_{k,h}(\boldsymbol{y}) \left[\frac{\delta_{ik}}{r} - r_{,ik} \right] dS_x\, dS_y$$
$$= \int_\Gamma \int_\Gamma \left[\tilde{\phi}_{i,h}(\boldsymbol{x})\phi_{i,h}(\boldsymbol{y}) \frac{1}{r} + (\tilde{\phi}_i(\boldsymbol{x}) - \tilde{\phi}_i(\boldsymbol{y}))(\phi_k(\boldsymbol{y}) - \phi_i(\boldsymbol{x})) r_{,ikhh} \right] dS_x\, dS_y$$
$$= \int_\Gamma \int_\Gamma [\tilde{\phi}_{i,h}(\boldsymbol{x})\phi_{i,h}(\boldsymbol{y}) - \tilde{\phi}_{i,i}(\boldsymbol{x})\phi_{k,k}(\boldsymbol{y})] \frac{1}{r}\, dS_x\, dS_y \tag{A.9}$$

noticing that $r_{,hh} = 1/r$ and

$$\int_\Gamma \int_\Gamma \tilde{\phi}_{3,f}(\boldsymbol{x})\phi_{3,h}(\boldsymbol{y}) \frac{r_{,f} r_{,h}}{r}\, dS_x\, dS_y = -\int_\Gamma \int_\Gamma \tilde{\phi}_{3,f}(\boldsymbol{x})(\phi_3(\boldsymbol{y}) - \phi_3(\boldsymbol{x})) \left(\frac{r_{,f} r_{,h}}{r} \right)_{,h} dS_x\, dS_y = 0 \tag{A.10}$$

since

$$\left(\frac{r_{,f} r_{,h}}{r} \right)_{,h} = \frac{r_{,fh} r_{,h}}{r} + \frac{r_{,f} r_{,hh}}{r} - \frac{r_{,f} r_{,h} r_{,h}}{r^2} = 0 + \frac{r_{,f}}{r^2} - \frac{r_{,f}}{r^2} = 0$$

Substitution of (A.8), (A.9), (A.10) into (A.7) finally yields the desired result (62).

A.4. Modified shape functions for the 9-noded boundary element

A.4.1. Modified shape function $\tilde{N}(\rho, \varphi; \boldsymbol{\eta})$

The usual shape functions are products of one-dimensional quadratic shape functions (69):

$$N(\xi_1, \xi_2) = S_i(\xi_1) S_j(\xi_2)$$

Introducing the variables (ρ, ϕ) defined by (82), the latter are readily seen to verify:

$$S_1(\xi_1) - S_1(\eta_1) = \rho \cos\varphi (\xi_1 + \eta_1 - 1)/2$$
$$S_1(\xi_2) - S_1(\eta_2) = \rho \sin\varphi (\xi_2 + \eta_2 - 1)/2$$
$$S_2(\xi_1) - S_2(\eta_1) = -\rho \cos\varphi (\xi_1 + \eta_1)$$
$$S_2(\xi_2) - S_2(\eta_2) = -\rho \sin\varphi (\xi_2 + \eta_2)$$
$$S_3(\xi_1) - S_3(\eta_1) = \rho \cos\varphi (\xi_1 + \eta_1 + 1)/2$$
$$S_3(\xi_2) - S_3(\eta_2) = \rho \sin\varphi (\xi_2 + \eta_2 + 1)/2$$

Noticing that

$$N(\xi_1, \xi_2) - N(\eta_1, \eta_2) = S_i(\xi_1)[S_j(\xi_2) - S_j(\eta_2)] + [S_i(\xi_1) - S_i(\eta_1)] S_j(\eta_2)$$

the modified shape functions defined by (83) are then readily obtained.

A.4.2. Modified vector shape functions $\hat{\boldsymbol{B}}^k(\rho, \varphi; \boldsymbol{\eta})$

$$\boldsymbol{B}^k(\boldsymbol{\xi}) = b^k(\xi)\boldsymbol{\nu}(\xi) \quad \text{with} \quad b^k(\boldsymbol{\xi}) = 1/2(1-\xi_2)S_k(\xi_1) \qquad \boldsymbol{\nu}(\boldsymbol{\xi}) = \frac{\boldsymbol{a}_1}{|\boldsymbol{a}_1|} \wedge \boldsymbol{n}$$

Using the natural basis $(\boldsymbol{a}_1, \boldsymbol{a}_2)$, one has

$$\boldsymbol{\nu}(\boldsymbol{\xi}) = e_{\alpha\beta}\boldsymbol{a}_\alpha(\boldsymbol{\xi})A_\beta(\boldsymbol{\xi}) \quad \text{with} \quad A_\beta(\boldsymbol{\xi}) = \frac{g_{1\beta}(\boldsymbol{\xi})}{\sqrt{g_{11}(\boldsymbol{\xi})\hat{g}(\boldsymbol{\xi})}} \tag{A.11}$$

One then has

$$\boldsymbol{B}^k(\boldsymbol{\xi}) - \boldsymbol{B}^k(\boldsymbol{\eta}) = [b^k(\boldsymbol{\xi}) - b^k(\boldsymbol{\eta})]\boldsymbol{\nu}(\boldsymbol{\xi}) + b^k(\boldsymbol{\eta})[\boldsymbol{\nu}(\boldsymbol{\xi}) - \boldsymbol{\nu}(\boldsymbol{\eta})]$$

which gives

$$\hat{B}_j^k(\rho, \varphi, \boldsymbol{\eta}) = \hat{b}^k(\rho, \varphi; \boldsymbol{\eta})\boldsymbol{\nu}(\boldsymbol{\xi}) + b^k(\boldsymbol{\eta})\hat{\boldsymbol{\nu}}(\rho, \varphi, \boldsymbol{\eta})$$

having put

$$b^k(\boldsymbol{\xi}) - b^k(\boldsymbol{\eta}) = \rho\hat{b}^k(\rho, \varphi; \boldsymbol{\eta}) \qquad \boldsymbol{\nu}(\boldsymbol{\xi}) - \boldsymbol{\nu}(\boldsymbol{\eta}) = \rho\hat{\boldsymbol{\nu}}(\rho, \varphi, \boldsymbol{\eta})$$

From expression (A.11) of $\boldsymbol{\nu}(\boldsymbol{\xi})$, one then obtains

$$\hat{\boldsymbol{\nu}}(\rho, \varphi, \boldsymbol{\eta}) = \{\hat{\boldsymbol{a}}_\alpha(\rho, \varphi; \boldsymbol{\eta})A_\beta(\boldsymbol{\xi}) + \boldsymbol{a}_\alpha(\boldsymbol{\eta})\hat{A}_\beta(\rho, \varphi; \boldsymbol{\eta})\}e_{\alpha\beta}$$

with

$$\rho\hat{A}_\alpha(\rho, \varphi; \boldsymbol{\eta}) = A_\alpha(\boldsymbol{\xi}) - A_\alpha(\boldsymbol{\eta}) \qquad \rho\hat{\boldsymbol{a}}_\alpha(\rho, \varphi; \boldsymbol{\eta}) = \boldsymbol{a}_\alpha(\boldsymbol{\xi}) - \boldsymbol{a}_\alpha(\boldsymbol{\eta})$$

Finally, explicit formulas for $\hat{\boldsymbol{a}}_\alpha(\rho, \varphi; \boldsymbol{\eta})$, $\hat{A}_\alpha(\rho, \varphi; \boldsymbol{\eta})$ and $\hat{b}^k(\rho, \varphi, \boldsymbol{\eta})$ are obtained by introducing the change of variables (82) and factoring out ρ.

References

[1] P. Berest, Q.S. Nguyen and R.M. Pradeilles-Duval, Stability and bifurcation of plane cracks of arbitrary shape, in: Computational Modelling of Free and Moving Boundary Problem (Comput. Mech. Publ., Southampton, 1993) 409–418.

[2] M. Bonnet, Méthode des équations intégrales régularisées en élastodynamique tridimensionnelle, Ph.D. Thesis, Ecole Nationale des Ponts et Chaussées, Paris (Nov. 1986), publiée dans le Bulletin EDF/DER série C, 1/2, 1987.

[3] M. Bonnet, Equations intégrales et éléments de frontière, CNRS Editions/Eyrolles, Paris, France, 1995.

[4] M. Bonnet, Regularized BIE formulations for first- and second-order shape sensitivity of elastic fields, Comput. Struct. 56 (1995) 799–811. (Invited paper, special issue, S. Saigal, guest editor).

[5] M. Bonnet, Regularized direct and indirect symmetric variational BIE formulations for three-dimensional elasticity, Engrg. Anal. Bound. Elem. 15 (1995) 93–102.

[6] M. Bonnet, G. Maier and C. Polizzotto, On symmetric Galerkin boundary element method, Appl. Mech. Rev. 51 (1998) 669–704.

[7] T.A. Cruse, Boundary Element Analysis in Computational Fracture Mechanics (Kluwer Academic Publishers, 1988).

[8] T.A. Cruse and P.M. Besuner, Residual life prediction for surface cracks in complex structural details, J. Aircraft 12 (1975) 369–375.

[9] H.G. Delorenzi, On the energy release rate and the *J*-integral for 3-D crack configurations, Int. J. Fract. 19 (1982) 183–194.

[10] Ph. Destuynder, M. Djaoua and S. Lescure, Quelques remarques sur la mécanique de la rupture élastique, J. Mécan. Théor. Appl. 2 (1983) 113–135.

[11] B. Doubrovine, S. Novikov and A. Fomenko, Géométrie contemporaine, méthodes et applications (première partie: géométrie des surfaces, des groupes de transformations et des champs) (Editions de Moscou, 1979).

[12] T.K. Hellen, On the method of virtual crack extension, Int. J. Numer. Methods Engrg. 9 (1975) 187–207.

[13] S. Li, M.E. Mear and L. Xiao, Symmetric weak-form integral equation method for three-dimensional fracture analysis, Comput. Methods Appl. Mech. Engrg. 151 (1998) 435–459.

[14] P. Mialon, Calcul de la dérivée d'une grandeur par rapport à un fond de fissure par la méthode θ, Bulletin EDF/DER série c vol. 3, Electricité de France, 1987.

[15] J.C. Nedelec, Integral equations with non integrable kernels, Integral Equations and Operator Theory 5 (1982) 562–572.

[16] Q.S. Nguyen, Bifurcation and stablity of time-independent dissipative systems. Advanced course on bifurcation and stability of dissipative systems, CISM Lectures, Udine, Italy, 1991.

[17] Q.S. Nguyen, Bifurcation and stability in dissipative media (plasticity, friction, fracture), Appl. Mech. Rev. 47 (1994) 1–31.

[18] Q.S. Nguyen, C. Stolz and G. Debruyne, Energy methods in fracture mechanics: stability, bifurcation and second variations, Engrg. Struct. 9 (1990) 157–173.
[19] N. Nishimura and S. Kobayashi, A boundary integral equation method for an inverse problem related to crack detection, Int. J. Numer. Methods Engrg. 32 (1991) 1371–1387.
[20] K. Ohtsuka, Generalized *J*-integral and three-dimensional fracture mechanics, Hiroshima Math. J. 11 (1981) 21–52.
[21] D.M. Parks, A stiffness derivative finite element technique for determination of crack tip stress intensity factors, Int. J. Fract. 10 (1974) 487–501.
[22] H. Petryk and Z. Mroz, Time derivatives of integrals and functionals defined on varying volume and surface domains, Arch. Mech. 38 (1986) 694–724.
[23] S. Sirtori, G. Maier, G. Novati and S. Miccoli, A Galerkin symmetric boundary element method in elasticity: formulation and implementation, Int. J. Numer. Methods Engrg. 35 (1992) 255–282.
[24] J. Sokolowski and J.P. Zolesio, Introduction to shape optimization. Shape sensitivity analysis, Vol. 16 of Springer Series in Computational Mathematics (Springer-Verlag, 1992).
[25] X.Z. Suo and A. Combescure, Sur une formulation mathématique de la dérivée de l'énergie potentielle en théorie de la rupture fragile, C.R. Acad. Sci. Paris, série II 308 (1122–1989) 1119.
[26] H. Tada, P. Paris and G. Irwin, The stress analysis of cracks handbook, Tech. Rep., Del. Research Corporation, Hellertown, Pennsylvania, USA, 1973.
[27] Y. Wadier and O. Malak, The theta method applied to the analysis of 3D-elastic-plastic cracked bodies, in SMIRT Proceedings, 1989.